Diploma Thesis

Preoperative Detection of Deep Inferior Epigastric Perforators
A Local Assessment by Various Appliances

submitted by

Simon Gatterer

In Fulfilment of the Requirements for the Degree of

Doctor medicinae universae

(Dr. med. univ.)

at the

Medical University of Graz

conducted at the

Department of Surgery

Division of Plastic, Aesthetic and Reconstructive Surgery

under the supervision of

Dr. med. univ. Hanna Luze

Univ. Prof. Dr. med. Lars-Peter Kamolz MSc.

Graz, 19.11.21

Statutory Declaration

I hereby declare that I have authored this diploma thesis fully on my own, that I have not used any other than the declared sources, and that I have explicitly marked all material which has been quoted either literally or by content from the used sources.

Graz, 19.11.21 *Simon Gatterer eh.*

Acknowledgments

First, I would like to thank Prof. Lars-Peter Kamolz, who primarily gave me the opportunity to take part in this study and who also supervised my thesis.
I am also very grateful to Dr. Hanna Luze, who supervised and assessed my thesis. I really appreciate her helpful suggestions and constructive criticism during the preparation of this work. Without her support and patience, my thesis would not have been possible. Further, I would like to thank Dr. Sebastian Nischwitz, who initially led this project and gave me valuable input for my work.
Additionally, I would like to thank my colleagues at COREMED, who assisted me during the research phase of this work and provided insights into the corporate culture.
Furthermore, I would like to thank my parents and sisters, who made it possible for me to study medicine and have always supported me throughout my academic career. Thank you for all the kind and motivating words, the backing, and the encouragement.
Lastly, I would like to thank the friends and colleagues with whom I spent the last six years and who made this time unforgettable. Thank you for all the interesting discussions, the study sessions, and the activities we shared.

Table of Contents

Statutory Declaration i
Acknowledgments ii
Table of Contents iii
Abbreviations iv
Figures v
Tables v
Zusammenfassung vi
Abstract viii
Publications x
1 Introduction 1
1.1 Background 1
1.2 Aim 3
1.3 Perforators 4
1.4 Breast reconstruction after mastectomy 5
1.4.1 Alloplastic reconstruction 5
1.4.2 Autologous reconstruction 7
1.5 Modern imaging technologies 16
1.5.1 Thermal imaging 16
1.5.2 Hyperspectral imaging 17
1.5.3 Laser Doppler imaging 17
2 Materials and methods 19
2.1 Study design 19
2.2 Study cohort 19
2.3 Detection devices 20
2.4 Study methods 21
2.5 Analysis 25
2.5.1 Statistical analysis 25
3 Results 26
3.1 Subject data 26
3.2 Overview 27
3.3 Thermal imaging results 28
3.4 Hyperspectral imaging results 29
3.5 Laser Doppler imaging results 30
4 Discussion 32
4.1 The use of thermal imaging in the medical field 32
4.2 Thermal imaging in the present study 33
4.2.1 Practicability of the FLIR One® 34
4.3 The use of hyperspectral imaging in the medical field 35
4.4 Hyperspectral imaging in the present study 36
4.4.1 Practicability of the TIVITA® Wound hyperspectral camera 37
4.5 The use of laser Doppler imaging in the medical field 37
4.6 Laser Doppler imaging in the present study 38
4.6.1 Practicability of the moorLDLS-BI LaserDoppler 38
4.7 Limitations and outlook 38
5 Conclusion 40
References 41

Abbreviations

ADM ..... *acellular dermal matrix*
ALT ..... *anterior lateral thigh*
BCT ..... *breast-conserving therapy*
BMI ..... *body mass index*
CT ..... *computed tomography*
DIEA ..... *deep inferior epigastric artery*
DIEP ..... *deep inferior epigastric perforator*
DNA ..... *deoxyribonucleic acid*
EIA ..... *external iliac artery*
HSI ..... *hyperspectral imaging*
IGAP ..... *inferior gluteal artery perforator*
LDI ..... *laser doppler imaging*
MR ..... *magnetic resonance*
NIR ..... *near infrared*
PAD ..... *peripheral artery disease*
PAP ..... *profunda artery perforator*
ROI ..... *region of interest*
SD ..... *standard deviation*
SGAP ..... *superior gluteal artery perforator*
SIEA ..... *superficial inferior epigastric artery*
TI ..... *thermal imaging*
TRAM ..... *transverse rectus abdominis myocutaneous*

Figures

Figure 1: Types of perforators according to *Blondeel et al.*. 4
Figure 2: Positioning of breast implants after mastectomy using ADMs. 6
Figure 3: Anatomy of the inferior epigastric vessels. 8
Figure 4: Anatomical depiction of perforators of the DIEA. 9
Figure 5: Right (short arrow) and left (long arrow) perforators of the DIEA in a preoperative CT. 10
Figure 6: The major perforator is identified 12
Figure 7: Overview of the surgical procedure. 13
Figure 8: FLIR One® Pro 20
Figure 9: TIVITA® Wound 20
Figure 10: Moor LDLS-BI LaserDoppler 21
Figure 11: The ROI 22
Figure 12: Imaging order group 1 23
Figure 13: Imaging order group 2. 24
Figure 14: Imaging order group 3 24
Figure 15: Summary of the detection results of the three imaging methods. 28
Figure 16: Exemplary depiction of a marked perforator and the corresponding perforator in the TI image 29
Figure 17: Exemplary depiction of a marked perforator and the corresponding perforator in the HSI image. 30
Figure 18: Exemplary depiction of a marked perforator and the corresponding LDI images, where no perforator was detectable. 31

Tables

Table 1: Data of the study population 27
Table 2: Correlation between body parameters and possible perforator detection via TI 29
Table 3: Correlation between body parameters and possible perforator detection via HSI 30

Zusammenfassung

Einleitung: Brustkrebs gehört zu den am weitesten verbreiteten Krankheiten in Europa und stellt den größten Anteil der bösartigen Erkrankungen der Frau dar. Die einzige kurative Therapie ist die chirurgische Resektion des entarteten Gewebes, die oft durch eine Bestrahlung oder Chemotherapie ergänzt wird. Bei ca. ca. 40% der Brustkrebspatientinnen kann keine brusterhaltende Therapie, sondern nur eine vollständige Resektion des Brustdrüsengewebes (subkutane Mastektomie) durchgeführt werden. Vor allem für diese Patientinnengruppe ist die durch die Erkrankung und Therapie verursachte psychologische und körperliche Belastung oft enorm, und auch nach erfolgreicher Behandlung kann das Fehlen der Brust erhebliche negative psychosoziale Effekte haben. Die plastisch-chirurgische Rekonstruktion der Brust ist daher eine Möglichkeit, den Betroffenen wieder zu mehr Selbstvertrauen und weiblicher Identifikation zu verhelfen.

Die Techniken der Brustrekonstruktion sind vielfältig und reichen vom Einsatz von Implantaten bis hin zur Transplantation von Eigengewebe. Bei Letzterem gilt der sogenannte DIEP-Lappen (deep inferior epigastric perforator flap) als aktueller Goldstandard. Dabei wird überschüssiges Haut- und Fettgewebe vom Bauch an die Brust mikrochirurgisch transferiert, um dort für eine natürliche und ästhetische Projektion zu sorgen. Eine große Rolle spielen dabei die sogenannten Perforator-Gefäße, die das Lappengewebe zu versorgen.

Um Komplikationen zu minimieren und ein optimales Ergebnis garantieren zu können, ist es für die behandelnden Chirurginnen und Chirurgen unabdingbar, die individuelle Gefäßanatomie sowie die dominanten Perforator-Gefäße der Patientin präoperativ exakt zu evaluieren. Hierfür gilt die CT-Angiographie als aktueller Goldstandard. Allerdings ist diese Methode invasiv, aufwendig und kann in vielen Fällen aufgrund von Vorerkrankungen nicht durchgeführt werden. Oftmals wird als Ergänzung zu dieser Technik der Stift-Doppler zur direkten Evaluierung an der Patientin eingesetzt, welcher allerdings keine visuelle Darstellung der Gefäße ermöglicht.

Im Rahmen dieser Arbeit wurden drei nicht-invasive und für den menschlichen Körper unschädliche Bildgebungsverfahren getestet, um mögliche Ergänzungen oder Alternativen für die oben genannten Verfahren zu evaluieren. Die eingesetzten Techniken umfassen die Bildgebung mittels Wärmebildkamera, Hyperspektralkamera sowie eines Laser-Doppler-Systems.

Methodik: Das vorliegende klinische Pilotprojekt wurde an der Klinischen Abteilung für Plastische, Ästhetische und Rekonstruktive Chirurgie, Universitätsklinik für Chirurgie der Medizinischen Universität Graz durchgeführt. An insgesamt 18 ProbandInnen wurden nach je 20-minütiger Kühlung des Bauches jeweils alle drei Technologien hinsichtlich einer möglichen Perforatordetektion getestet und die Resultate mit Referenzperforatoren, die mittels Stift-Doppler eruiert wurden, verglichen. Zusätzlich wurden körperliche Charakteristika wie Alter, Geschlecht, BMI und Bauchumfang erhoben. Die Ergebnisse wurden statistisch ausgewertet.

Ergebnisse: Mit einer Sensitivität von 92,59 % erzielte die Wärmebildkamera die höchste Detektionsrate, gefolgt von der Hyperspektralkamera mit 25,93 %. Mittels Laser-Doppler-System konnte kein Perforator detektiert werden, was somit eine Sensitivität von 0% ergab. Unabhängig von der angewendeten Technologie zeigten sich keine Korrelationen der Detektionsraten mit Alter, Geschlecht, BMI oder Bauchumfang.

Diskussion/Schlussfolgerung: Von den evaluierten Geräten konnte nur die Wärmebildkamera eine zufriedenstellende Detektionsrate erreichen. Da die Wärmebildkamera nicht nur praktikabel und handlich, sondern auch kostengünstig ist, kann diese Technologie hervorragend im klinischen Alltag als Ergänzung in der präoperativen Perforatordetektion eingesetzt werden. Um das volle Potential von Wärmebildkameras zur Perforatordetektion zu evaluieren, sind Folgestudien mit größeren Patientenkohorten von größter Wichtigkeit.

Abstract

Introduction: Breast cancer is the commonest malignancy in the world and is the most frequent type of cancer in women. On average, one in eight women will develop breast cancer during their lifetime. The only curative therapy is surgical resection of the degenerated tissue, often supplemented with radiation or chemotherapy. In about 40% of breast cancer patients, breast conserving therapy is not possible, leading to subcutaneous mastectomy as the only remaining option. Especially for those patients, the psychological and physical stress triggered by the disease and therapy is often enormous, and even after successful treatment, the absence of the breast can have negative psychosocial effects. Breast reconstruction is therefore a way to help sufferers regain greater self-confidence, well-being, and female identification.

Breast reconstruction techniques are diverse and range from the use of implants to the transplantation of autologous tissue. In the latter, the deep inferior epigastric perforator (DIEP) flap is the current gold standard and is used by many surgeons worldwide with excellent results. In this procedure, excess skin and subcutaneous adipose tissue is transplanted from the abdomen to the breast to provide a natural and aesthetic projection. A key role is played by the so-called perforator vessels, which branch off from larger, deeper vessels to supply the flap tissue.

To ensure an optimal result in the reconstruction, it is essential for the surgeon to know the patient's individual vascular anatomy and thus plan the operation in the most viable way. CT angiography is the current gold standard for preoperative perforator detection. However, this method is expensive, time-consuming and cannot be performed in many cases because it requires a contrast medium, which can cause allergic reactions and renal failure.

In this work, three non-invasive imaging techniques that are harmless to the human body were tested to search for alternatives to CT angiography. The techniques involved a thermal camera, a hyperspectral camera, and a laser Doppler system.

Methods: This pilot project was performed in 18 subjects at the Division of Plastic, Aesthetic and Reconstructive Surgery, Department of Surgery, Medical University of Graz, Austria. After cooling the abdomen for 20 minutes, the three technologies were tested for their ability to detect perforators. The results were compared and matched with reference perforators obtained by using a pencil Doppler. The results were then statistically analyzed.

Results: Thermal imaging achieved the highest detection rate with a sensitivity of 92.59%, followed by the hyperspectral camera with 25.93%. The laser Doppler system was unable to detect a single perforator and therefore achieved 0% sensitivity. Regardless of the technology used, there were no correlations of detection rates with age, sex, BMI, or abdominal circumference.

Discussion/Conclusion: Of the devices used, only the thermal imaging camera achieved a satisfactory detection rate. As this device was also effective in terms of practicality and handiness and can be used independently of individual health data, this technology is a viable additional technology to conventional techniques.

Thermal imaging may particularly be used as a valuable alternative in patients where CT angiography is not possible. However, follow-up studies with larger patient cohorts are needed to evaluate the full potential of thermal imaging for perforator detection.

Publications

Nischwitz SP, Luze H, Schellnegger M, Gatterer SJ, Tuca A-C, Winter R, et al. Thermal, Hyperspectral, and Laser Doppler Imaging: Non-Invasive Tools for Detection of The Deep Inferior Epigastric Artery Perforators—A Prospective Comparison Study. J Pers Med 2021, Vol 11, Page 1005. 2021 Oct 5 [cited 2021 Oct 20];11(10):1005. Available from: https://www.mdpi.com/2075-4426/11/10/1005/htm

Since this publication is based on the same project as the following thesis, overlaps of content and wording may be found to a certain degree.

1 Introduction

1.1 Background

Breast cancer is the commonest malignancy in the world and is the most frequent type of cancer in women (1). In 2020, more than 2.2 million women worldwide were newly diagnosed with malignant neoplasms in the breast tissue, representing 24.5% of all new cancers in women (2). The lifetime risk is 12.4 %, meaning 1 in 8 women will develop breast cancer (3).

The only established curative therapy for breast cancer is surgical excision. According to the respective tumor, this is generally combined with radiation therapy, chemotherapy, targeted therapy, and/or hormonal therapy (4). Depending on the size, location, and staging of the tumor, the surgery itself can be performed either as breast-conserving therapy (BCT) or complete removal of the mammary gland (mastectomy) (5).

If a BCT is possible, a lumpectomy is performed, where the tumor and a small, cancer-free margin of healthy tissue surrounding it is resected while the majority of the breast tissue is conserved. In about 40% of breast cancer patients, BCT is not possible because of insufficient histological resection margins, tumor multifocality, or too large a tumor relative to the patient's breast size (6). In these cases, a subcutaneous mastectomy is required. Mastectomy is the removal of the entire breast tissue and can be performed using various techniques, including a skin-sparing mastectomy—which, as the name suggests, preserves the maximum amount of skin—and a nipple-sparing mastectomy, where the areola and the nipple are conserved.

In addition to the burden of breast cancer surgery, getting diagnosed with breast cancer is challenging for women in many psychosocial aspects. There is the confrontation with the disease itself. Patients become aware of their mortality, and nearly 50% of those affected develop depression or anxiety (7). They must also face exhausting and demanding therapies before and after surgery, which may include chemotherapy and/or radiotherapy. The results of these therapies, especially the ablation of the breast, is often unsatisfactory in terms of aesthetics and is viewed by the patient as a physical impairment (8). Since the female breast is a visible symbol of female identity, attractiveness, and socioemotional acceptance, many patients who have undergone mastectomy suffer body-image issues (ibid.). According to

Benditte-Klepetko et al. (2003), the feminine self-perception of women who had a breast removed due to cancer is severely affected, but it can be significantly restored in 85% of cases if surgical reconstruction is performed (9). This circumstance suggests that breast reconstruction is a vital step in treating patients who have lost their breast to cancer if they are to regain full physical and mental health.

There are several techniques used for breast reconstruction. The two main methods are implant-based alloplastic reconstruction and autologous reconstruction, where the patient's own tissue is used to reconstruct volume and shape of the breast. (*cf. Section 1.4*)

Advantages of alloplastic reconstruction include shorter surgery duration, faster healing, and far-reaching applicability. However, the implants can cause complications, such as capsular contracture, which is the excessive formation of (shrinking) scar tissue around the implant, causing pain, discomfort, and aesthetic impairment (10).

The autologous reconstruction provides a more natural look, greater physical sensitivity, and a significantly higher degree of satisfaction in terms of aesthetics, psychosocial well-being, and sexual well-being (11). The downside of this technique is the significantly longer duration of the surgical procedure and the more extended healing period.

Different methods can be used within the autologous reconstruction technique, depending on the patient's anatomical circumstances and wishes. These methods include pedicled flaps, where the original supplying vessel of the transferred tissue is conserved (e.g., latissimus dorsi flap and pedicled transverse rectus abdominis myocutaneous [TRAM] flap), and free flaps, where the original supplying vessel of the flap is detached from the donor site and microsurgically connected to another vessel in the recipient area.

The deep inferior epigastric perforator (DIEP) flap is a prime example of the latter. It is the gold standard in autologous breast reconstruction and is increasingly used by many surgeons worldwide (12,13). The benefits of the technique include minimal donor site morbidity, natural appearance and favorable aesthetic results.

To provide the best possible outcome in this surgery, it is necessary to know the individual vascular anatomy of the abdominal wall of each patient prior to the surgery since the location of perforator vessels can significantly vary. Various appliances

can be used to detect these vessels, with CT and MR-angiography being the gold standard, providing detailed information about the vascular anatomy (14). However, these invasive procedures have disadvantages, including expense, the possibility of an adverse reaction to iodine contrast, and the damage to DNA through radiation (15).

Ultrasound devices such as the color Doppler, duplex sonography, and the handheld Doppler show satisfactory results and complement CT angiography findings. Furthermore, they are easy to use directly on the patient, inexpensive, and have no adverse effects. However, these procedures are often dependent on the examiner's experiences with the respective technique.

In addition to these procedures, there are new non-invasive imaging technologies that can be used to detect perforators and their angiosomes.

In this pilot study, three new techniques were tested for their ability to provide visual information on the individual vascular anatomy of the abdominal wall, including:

1. Thermal imaging
2. Hyperspectral imaging
3. Laser Doppler spectroscopy

The main reason for including these three technologies is the promising results reported in previous studies (c.f. *Section 1.5*). Furthermore, all these procedures are non-invasive and non-harmful to the human body (e.g., through radiation).

The specificity and sensitivity were determined by the ability of each technology to locate perforator vessels that were previously identified and marked using an acoustic handheld pencil Doppler device.

1.2 Aim

The aim of this work was to test the usefulness and accuracy of the three named new preoperative imaging methods in detecting perforator vessels in the abdominal wall. These perforator vessels are essential for the blood supply of the DIEP flap but can anatomically vary from patient to patient. It is essential for the surgeon to examine their exact location pre-operatively to prevent intraoperative and postoperative complications and guarantee the best possible outcome.

1.3 Perforators

A perforator vessel, frequently abbreviated to perforator, is a vessel that originates in a larger axial vessel and runs through different tissues before reaching and thus supplying the subcutaneous fat tissue and the corresponding skin. *Hallock (2003)* roughly divides them into direct and indirect perforators according to the course they pursue (16). From a more surgical point of view, *Blondeel et al. (2003)* differentiate between five subtypes of perforators as displayed in *Figure 1* (17):

"1. Direct perforators perforate the deep fascia exclusively.

2.Indirect muscle perforators predominantly supply the subcutaneous tissues.

3. Indirect muscle perforators predominantly supply the muscle but have secondary branches to the subcutaneous tissues.

4. Indirect perimysial perforators travel within the perimysium between muscle fibers before piercing the deep fascia.

5. Indirect septal perforators travel through the intermuscular septum before piercing the deep fascia."

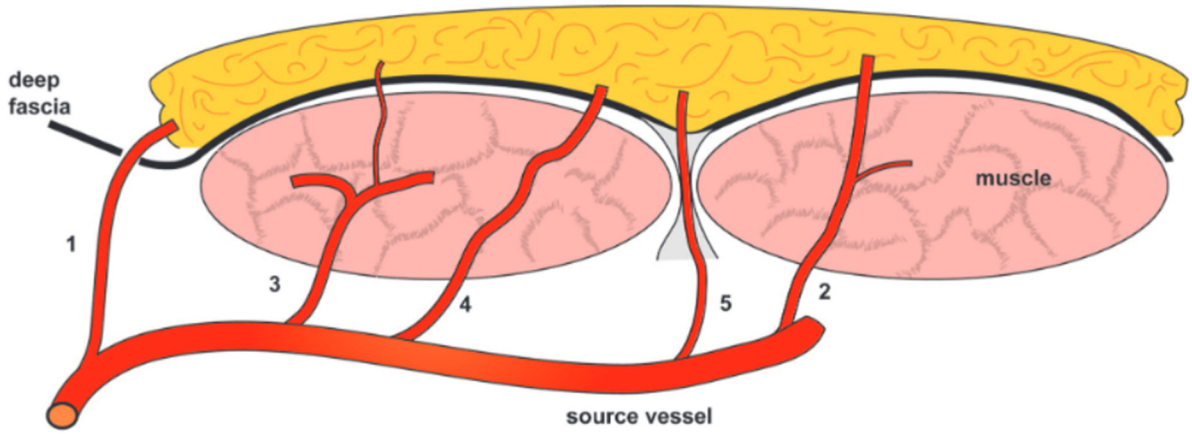

Figure 1: Types of perforators according to *Blondeel et al.*: a source vessel with different perforators. 1. Direct muscle perforators; 2, 3. Indirect muscle perforators; 4. Indirect perimysial perforators; 5. Indirect septal perforators (17)**.**

The abdominal wall used in the breast reconstruction procedure with free flaps is mainly supplied with blood through perforator vessels. These perforators arise from the inferior and superior epigastric arteries, which are connected through an anastomosis. The anatomy of these vessels is described in more detail in *Subsection 1.4.2.1.1*.

1.4 Breast reconstruction after mastectomy

Primarily, there are two options regarding the timing of breast reconstruction. It can be performed directly following the mastectomy (primary reconstruction) or in further surgery (secondary reconstruction). Hence, the decision is taken individually and depends on such factors as the necessity of radiotherapy following the surgery, which can lead to aesthetical impairments of the reconstructed breast.

In terms of oncological safety, it is inconsequential whether the reconstruction is done primarily or secondarily (18,19).

As mentioned in *Section 1.1*, two main techniques for breast reconstruction can be used: alloplastic and autologous reconstruction. Depending on the individual circumstances and the patient's wishes, the surgeon will recommend the method with the best possible outcome, sometimes even combining the above-mentioned techniques.

1.4.1 Alloplastic reconstruction

Implant-based reconstructions account for over 75% of reconstruction procedures following mastectomy (20). An implant is a flexible shell filled either with silicone or saline water, which can be placed under (subpectoral) or over (prepectoral) the pectoralis major muscle. Depending on the size and shape of the implant, breasts can be augmented and shaped individually. Discussion concerning the two placement options has been ongoing for a long time and opinion on the subject varies. Subpectoral implant placement has traditionally been perceived as the "safest" method with regard to rates of postoperative complications such as seroma, infection, and implant loss. However, in the last few years, prepectoral implant placement has become popular again as a less invasive alternative. Its advantages include minimization of animation deformity and reduced pain and discomfort (21).

To keep the implant in place, an acellular dermal matrix (ADM) is increasingly used. It can be used with prepectoral and subpectoral placement techniques, and it supports the position of the implant and effectively reduces the incidence of capsular contractures (22).

The two positioning possibilities of breast implants using ADMs are displayed in *Figure 2*.

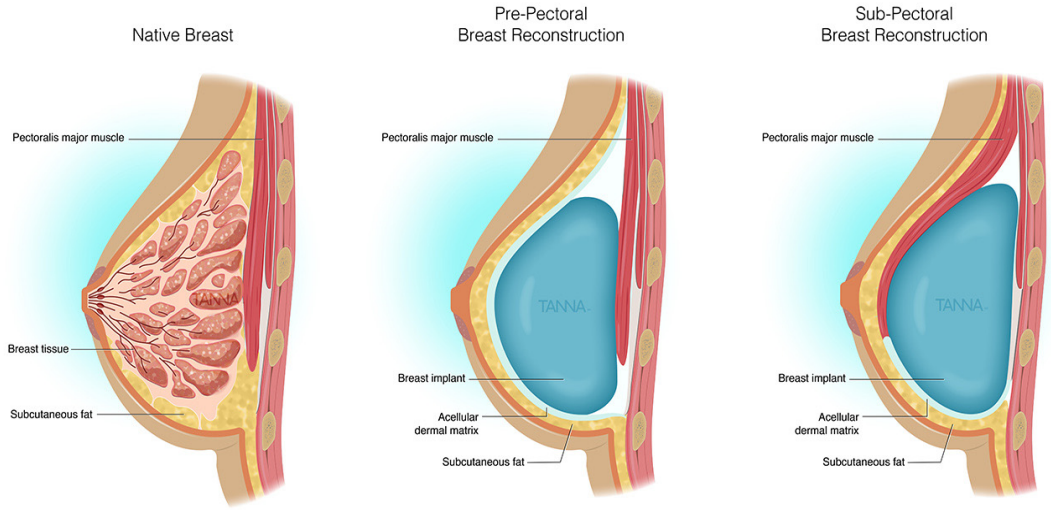

Figure 2: Positioning of breast implants after mastectomy using ADMs (23)**.** The position of the ADM varies, depending on the implant placement. If the implant is placed prepectoral, the ADM covers the entire front of the implant (middle). In submuscular implant placement, the ADM covers the bottom of the implant and is attached to the pectoralis major muscle on the front (right).

The alloplastic reconstruction can be performed immediately after mastectomy or in subsequent surgery. To place a breast implant primarily, an adequate amount of healthy skin needs to be available to ensure the closure of the incision (e.g., after a skin-sparing mastectomy). If there is not enough skin available, it is necessary to use a tissue expander to expand the skin tissue to cover the implant. A tissue expander is a soft shell that can be successively filled with saline water using a syringe. Through the slow expansion of the device, more skin is gained, and the tissue expander can then be replaced with an implant. This procedure ensures safe skin closure and more subtle scarring, as there is less strain on the wound's edges. The main advantages of alloplastic breast reconstruction in comparison with autologous breast reconstruction are as follows:

- Shorter and simpler surgery
- Faster recovery time
- No additional incisions/scars on the abdomen, buttocks, etc.

However, one of the disadvantages of this technique is the susceptibility of the implants and the surrounding tissue to radiotherapy-induced damage (24). Hence, it is recommended to carry out the implant-based reconstruction after radiotherapy has ended or use other techniques, such as autologous tissue transfer.

1.4.2 Autologous reconstruction

The second technique for breast reconstruction is the use of autologous tissue. There are various methods and donor sites that can be used for this procedure depending on the individual constitution. What they generally have in common is the transfer of autologous tissue from a donor site to the breast area.

A distinction is generally made between pedicled flaps and free flaps. While the original vessels that supply the flap with blood and oxygen are sustained in pedicled flaps, free flaps are entirely separated from their original blood supply at the donor site and microsurgically attached to different blood vessels in the breast area (= recipient site.)

From this fact, it can be concluded that the donor sites of pedicled flaps need to be in the immediate environment of the recipient site, whereas free flaps can be harvested from areas further away. Another distinction can be made between the types of tissue used. Some methods only use skin and the underlying subcutaneous fat, while others include muscle tissue (e.g., TRAM flap.)

The reasons for choosing to reconstruct the breast with autologous tissue rather than implants can vary individually and include the following factors:

- Insufficient tissue to cover or support an implant following mastectomy or radiotherapy
- Forthcoming or following radiotherapy (25)
- Personal reasons (e.g., the patient does not want foreign bodies implanted)
- Generally good outcomes and high patient satisfaction (11)

However, several factors limit the use of autologous techniques, including the absence of an adequate amount of tissue at the intended donor site, pre-existing scars that may have damaged the tissue or the supplying vessels, or previous failed flap surgery.

1.4.2.1 The DIEP Flap

Since the DIEP flap is of paramount importance in this work, it is described in more detail in this subsection.

The DIEP flap was first described by *Koshima et Soeda* in 1989 (26). As the name suggests, it is supplied with blood and oxygen through a perforator vessel of the deep inferior epigastric artery (DIEA). The purpose of the DIEP flap is to preserve the muscle tissue of the abdominal wall to minimize donor site morbidity. Ergo, the

DIEP flap is composed entirely of skin and subcutaneous fat tissue and the surgery is carried out only as a free tissue transfer.

In 2020, 68% of all reconstructive breast procedures performed by members of the American Society of Plastic Surgeons using autologous flaps were performed using DIEP flaps, making it by far the most common reconstructive breast surgery after implant-based reconstructions (20).

The procedure's popularity results from its combination of excellent outcomes in terms of aesthetics and donor site morbidity and the reliability and safety of the blood supply (27).

1.4.2.1.1 Anatomy

The DIEP flap is supplied with blood and oxygen through a perforator vessel of the DIEA. The DIEA originates from the external iliac artery (EIA) and provides a major part of the lower abdominal area with blood. It arises from the EIA immediately above the inguinal ligament and curves forward in the subperitoneal space, where it proceeds along the interfoveal ligament, accompanied by its concomitant veins (cf. *Fig.3*) (28). It then perforates the inner fascia of the transversal abdominis

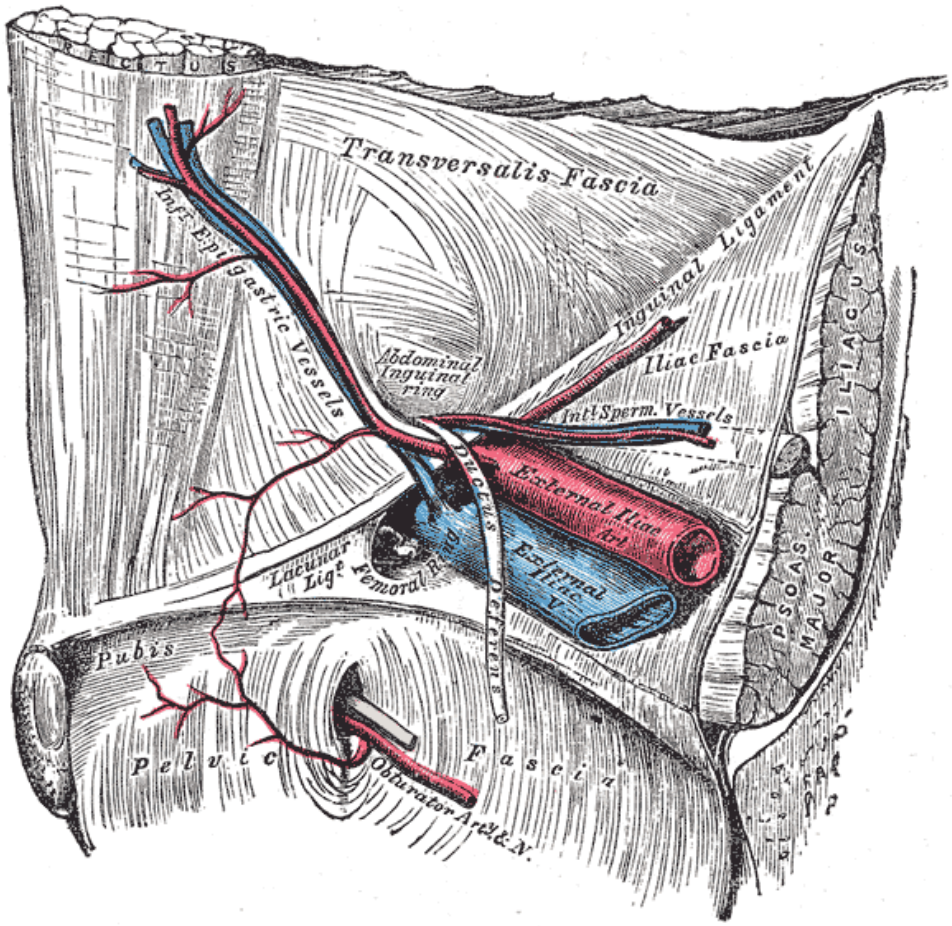

Figure 3: Anatomy of the inferior epigastric vessels, view from inside the abdomen (28).

muscle and continues to rise upward between the posterior rectus sheath and the rectus abdominis muscle, passing anteriorly of the arcuate line.

In this section of the artery, the DIEA establishes several perforators that pierce through the rectus abdominis muscle and supply it and the above-lying subcutaneous and skin tissue with blood (cf. *Fig. 4*).

Superior of the umbilicus, the DIEA splits into several smaller vessels that anastomose with the superior epigastric branch of the internal thoracic artery and the lower intercostal arteries.

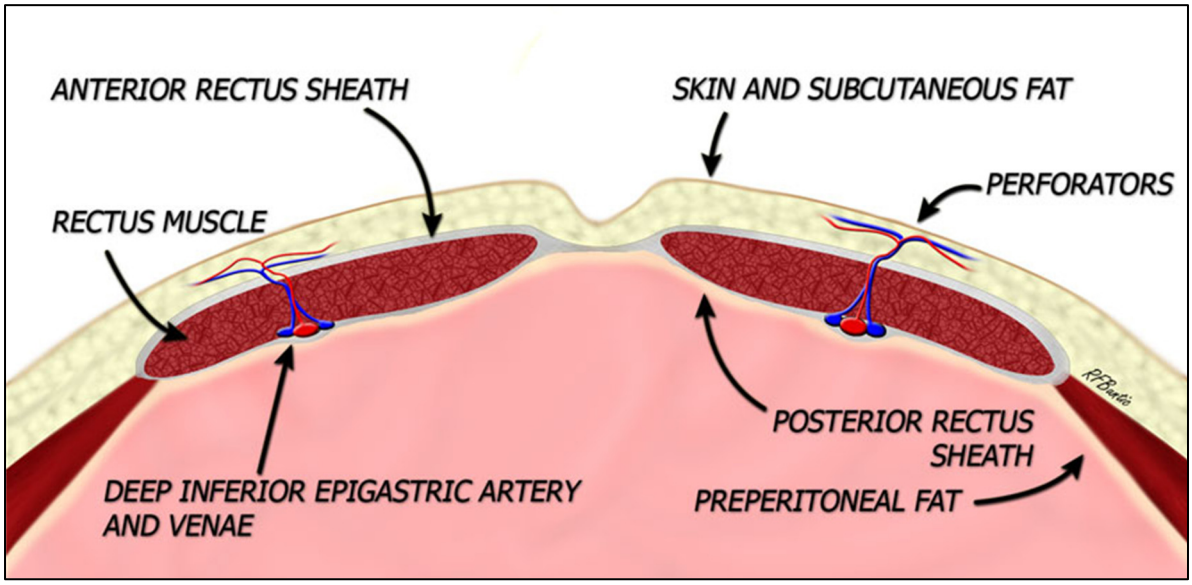

Figure 4: Anatomical depiction of perforators of the DIEA (29)**.**

Besides the perforator vessels, the DIEA establishes two side branches:

- The pubic branch, which anastomoses with the pubic branch of the obturator artery originating from the internal iliac artery, building the corona mortis
- The cremasteric artery in males, which supplies the spermatic cord and the cremaster muscles
- The artery of the round ligament of the uterus in females

1.4.2.1.2 Preoperative perforator detection

To minimize intraoperative and postoperative complications and provide the best possible outcome, it is crucial for the surgeon to examine the individual vascular anatomy of the abdominal wall of each patient prior to the surgery since the location of perforator vessels can significantly vary. Various appliances can be used to detect

those vessels. Invasive CT angiography is the current gold standard and provides detailed information about vascular anatomy (14). It is performed routinely in the preoperative procedure in many hospitals (cf. *Fig. 5*).

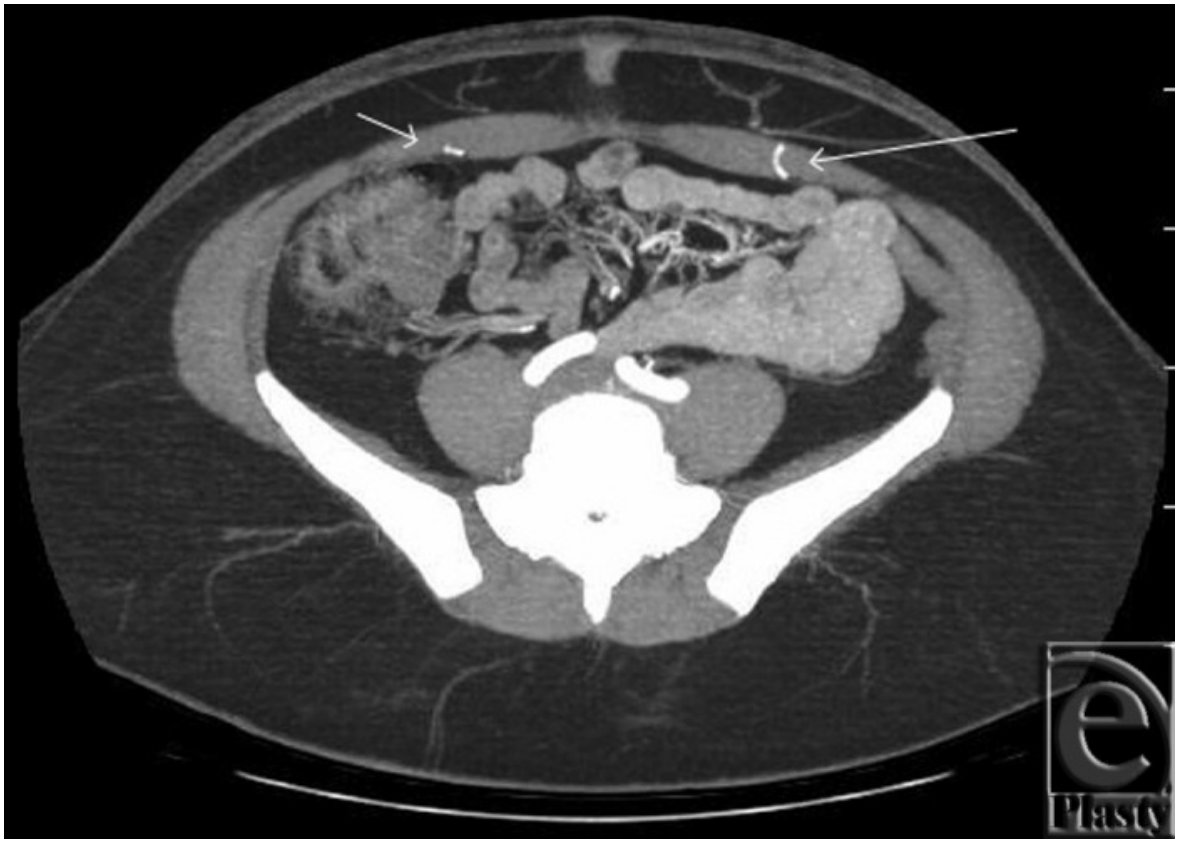

Figure 5: Right (short arrow) and left (long arrow) perforators of the DIEA in a preoperative CT (30)**.**

Ultrasound devices such as the color Doppler, duplex sonography, and the handheld Doppler show satisfactory results and can complement the findings of the CT angiography. Furthermore, they are easy to use directly on the patient, inexpensive, and have no adverse effects. In addition, several new imaging techniques have been introduced in the surgical field. These are not widespread yet, but they have the potential to assist in preoperative perforator screening (cf. *Section 1.5*).

Once the screening is completed, the detected perforators are marked with a surgical marker. Subsequently, to ascertain which perforator is most prominent and best suited for the flap, the markings can be numbered according to the findings in the imaging techniques (e.g., numeration according to loudness in pencil Doppler screening; 1 = loudest perforator, 2 = second loudest, etc.). Although only one

perforator is required for a sufficient blood supply, it is vital to mark other perforators in case of complications.

The intended flap design is then lined. The lower incision line is transversely placed superior to the pubic bone, extending laterally in a moderate upward curve above the inguinal ligament, ending shortly before the superior anterior iliac spines. The upper aspect of the incision starts above the umbilicus, curving gently downward to the ends of the lower line. To ensure that the wound's closure will not be too tight, a preoperative pinch test can be performed with the hip and knees moderately flexed (29). Lastly, the umbilical incision line is marked.

1.4.2.1.3 Surgical procedure

The surgery is commonly performed in general anesthesia and in the supine position. The patient's entire chest and abdominal area are cleaned with an antiseptic solution, and sterile surgical drapes are placed around the surgical site.

The surgery is usually performed in two teams simultaneously:

Team 1 prepares the recipient area on the chest by exciding the mastectomy scar (not necessary in primary reconstruction) and portraying the following supply vessels.

Team 2 performs the elevation of the DIEP flap from the lower abdomen.

Team 1: The pre-existing scar (in secondary reconstruction only) is excided extensively to obviate subsequent wound complications. The skin is detached from the fascia of the pectoralis major muscle, and a cavity for the placement of the DIEP flap is created. Next, the preparation of the supplying vessels for the microsurgical transfer is performed. For this purpose, the intercostal muscles are cut through, usually in the third, fourth, or fifth intercostal space (31,32). Another approach is the removal of a segment of costal cartilage of the rib to delineate the internal thoracic vessels more clearly. However, in some patients, cartilage removal may result in a visible medial chest-wall depression that requires corrective procedures afterwards (31).

After cutting through the intercostal muscles, the internal thoracic vessels (internal thoracic artery and vein) are displayed and prepared for the microsurgical anastomosis. Simultaneously, the DIEP flap is elevated by **team 2**.

The pre-drawn flap lines are incised, and the detachment of the subcutaneous fat tissue from the fascia beneath is begun, usually starting laterally. Progressing closer

to the marked perforators, increased cautiousness is required to avoid injuring the vessels (cf. *Fig. 6*).

Once the preferential perforator is displayed, the rectus fascia is incised longitudinally around the vessel. Exercising great care, it is traced through the muscle, clipping or coagulating small side branches of the perforator on the way. It is traced down to its origin, the deep inferior epigastric artery. This can result in a vascular pedicle of a length of more than 10cm.

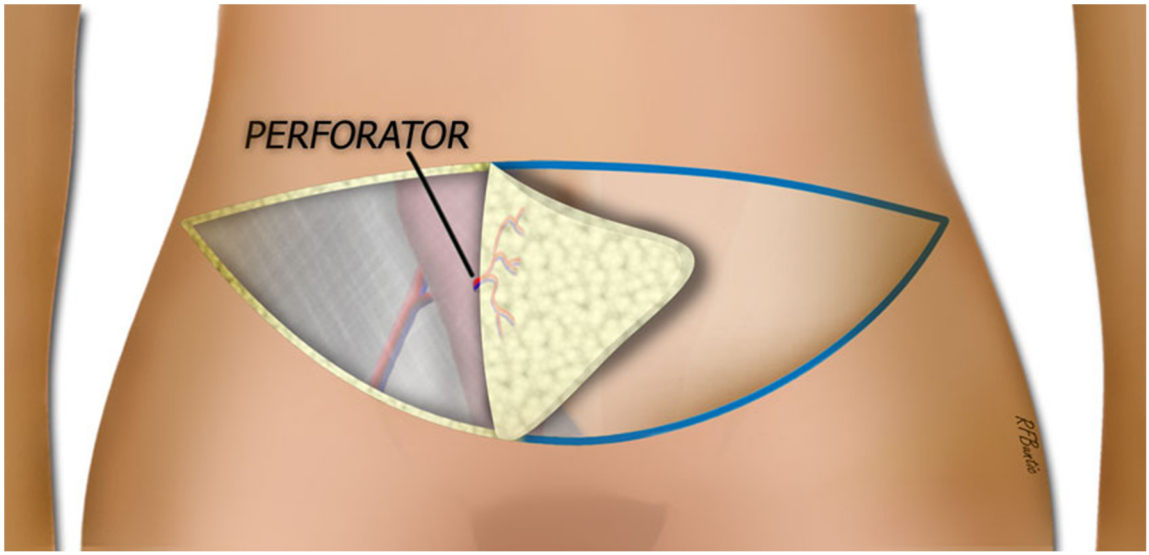

Figure 6: The major perforator is identified (29).

When the perforating artery and vein have been dissected down to the deep inferior epigastric vessels, it is time to detach the rest of the DIEP flap, sparing the umbilicus, which will be sutured into its new place later. During this process, other marked (or even unmarked) perforators can be found and are usually ligated to prevent excessive bleeding. After the entire flap is isolated on the intended perforator vessels and the recipient area is set, the DIEA and the venae can be clipped and surgically disconnected.

The DIEP flap is now placed in the prepared recipient area, and it is provisionally fixed in place using sutures. Next, the anastomoses of the internal thoracic artery and vein with the flap vessels are performed. An operating microscope is used for this purpose, which provides clear and sharply focused images. The flap vessels are primarily flushed with a heparin solution using microsurgical instruments to prevent the blood from forming clots, which could lead to flap loss. The anastomoses are performed using microsurgical sutures ranging from 9-0 to 12-0. The standard

material for these sutures is nylon, since it is easy to knot and produces minimal tissue reaction (33). Vascular clamps are frequently used to keep both ends of the vessels in place and prevent bleeding from the internal thoracic vessels. After completing the anastomoses, the clamps are released, and the perfusion is evaluated by reviewing the color, temperature, and capillary refill time. Other methods include employing a sterile pencil Doppler device or a visualization using indocyanine green as a fluorescent marker.

In the next step, the flap is trimmed and modeled to create a natural and sufficient projection of the newly created breast. This process individually varies from patient to patient. When a satisfactory result is achieved, the flap is sutured into place, and drains are placed, preventing blood or wound fluid from accumulating in the wound. Perfusion checks are performed repeatedly.

Simultaneously, the closure of the abdominal operating side is performed. The wound margins are brought together and sutured, and drains are placed once more.

In the next step, the new location of the umbilicus is determined and marked using a surgical marker. It is then passed through a V-shaped incision and sutured in place.

Lastly, the surgical wounds are bandaged, usually using paraffin gauze dressings covered by sterile gauze swabs. The abdomen is additionally covered with a bandage, applying mild pressure on the wound.

Figure 7 displays an overview of the operation sequence.

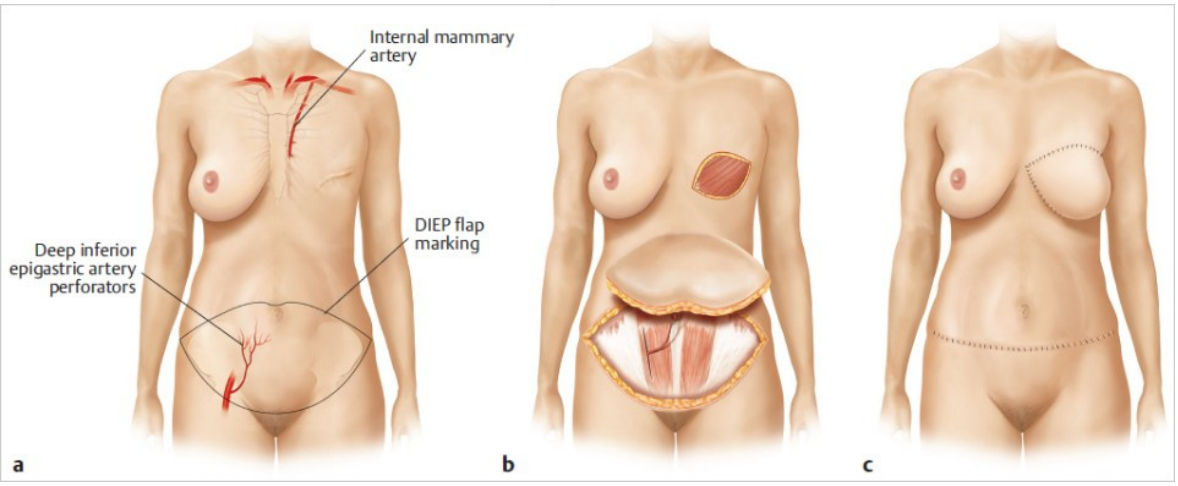

Figure 7: Overview of the surgical procedure (34)**.** a) Marking of the incision lines and visualization of the supplying vessels, b) Preparation of the donor site and elevation of the flap, c) completed breast reconstruction with a DIEP flap and postoperative scars.

Various alternatives for autologous breast reconstruction exist in addition to the DIEP flap. The main options are summarized in the following subsections.

1.4.2.2 The TRAM Flap

TRAM is an acronym for transverse rectus abdominis myocutaneous (flap). As the name suggests, the flap contains muscle tissue as well as skin and subcutaneous fat tissue. The TRAM flap can either be transferred as a pedicled flap or a free flap.

- Pedicled flap: During the surgery, a "skin tunnel" between the abdominal area and breast is created, through which the flap, which is still connected to its original supplying vessels (superficial and deep epigastric arteries), is transpositioned and then fixed in the recipient area.
- Free flap: The supplying vessels of the flap (usually a deep epigastric artery) are detached and microsurgically reconnected to its new vessels in the breast area (internal thoracic artery). This method is often called "muscle-sparing TRAM flap," as the transverse rectus abdominis is only dissected in the area of the supplying vessel.

A major disadvantage of this technique is the resulting disintegrity of the abdominal wall, which can lead to muscle weakness and hernias (35,36).

1.4.2.3 The SIEA Flap

This flap is located on the lower abdomen and is supplied with blood and oxygen by the superficial inferior epigastric artery (SIEA), which originates from the femoral artery below the inguinal ligament and runs toward the umbilicus between the fascia of Scarpa and the fascia of Camper (the two layers of the superficial abdominal fascia) (37).

The SIEA flap preserves the rectus abdominis muscle and uses only skin and subcutaneous fat tissue, which results in less postoperative pain and a faster recovery.

However, these vessels are not present in some patients, and even when present, their diameter is often too small to provide a reliable blood supply for a flap. This is one of the reasons why the SIEA flap is infrequently used, although some studies suggest it could be an appropriate choice in many reconstructive treatments (37).

1.4.2.4 SGAP/IGAP Flaps

The SGAP (superior gluteal artery perforator) and IGAP (inferior gluteal artery perforator) flaps use tissue from the gluteal area. This technique is mainly used in patients who do not have an adequate amount of tissue in other areas or present with pre-existing scars (e.g., after abdominoplasty) in the abdominal area.

As the name suggests, the SGAP and IGAP flaps use perforator vessels of the superior and inferior gluteal artery. Many surgeons favor the SGAP over the IGAP flap because the surgical site of the IGAP flap is placed near the sciatic tuber, which is a weight-bearing area while sitting. Therefore, choosing the IGAP flap can lead to postoperative pain and wound complications (38).

1.4.2.5 The PAP Flap

The profunda artery perforator (PAP) flap is located on the proximal and posterior-medial thigh and is supplied by perforators of the deep femoral artery. It can be designed either horizontally or vertically and consists of skin and subcutaneous fat tissue only. Along with the SGAP and IGAP flaps, this flap is primarily used for patients who do not have an adequate amount of tissue in the abdominal area or do not need a lot of volume at the recipient site (39).

1.4.2.6 The Latissimus Dorsi Flap

The latissimus dorsi flap is a musculocutaneous flap and is usually performed pedicled. Considering this circumstance, it is a viable option for patients who would normally be at risk of complications associated with reconstruction using free tissue transfer. Such patients include those with risk factors such as diabetes, hypertension, and smoking (40,41).

The latissimus dorsi flap is frequently used during breast reconstruction in combination with implants to give the breast a more natural appearance. The flap's dominant vessel is the thoracodorsal artery, a branch of the subscapular artery, but it is also perfused through perforators originating from the posterior intercostal arteries and the lumbar artery.

During the surgical procedure, a skin tunnel is created in the axillary area, through which the flap is transferred onto the chest.

1.5 Modern imaging technologies

Regarding preoperative perforator mapping, various new imaging technologies have been introduced to the medical and surgical fields so far. They allow medical professionals to visualize specific factors of the investigated area quickly and non-invasively. The three novel techniques assessed in this study are described in the following subsections.

1.5.1 Thermal imaging

Thermal imaging (TI), also known as infrared thermography, is a method of imaging that displays temperature by capturing infrared radiation emitted by objects and using this data to create images through digital or analog video outputs. Infrared is electromagnetic radiation with wavelengths longer than those of visible light. It is therefore invisible to the human eye. According to Planck's black body radiation law, every object above absolute zero emits infrared radiation that increases with temperature (42). Therefore, it is possible to differentiate warmer from colder objects or warmer from colder areas on the same object using a device that captures and processes infrared radiation (i.e., a thermal camera.)

This technology has been used successfully in many fields, including military, construction, firefighting, and geology. It has also been adopted by the medical field, helping with the diagnosis of such conditions as peripheral artery disease (PAD), neuro-musculoskeletal diseases, and, as relevant to this study, screening for perforator vessels prior to flap surgery (43,44). Further examples of its application in plastic surgery include the assessment of burn wounds and the postoperative monitoring of free flaps (45,46).

TI has increasingly become a factor in the preoperative detection of perforators since the early 2000s. It is considered a quick and easy procedure with a high detection rate (47). *Pereira et al. (2018)* found a "high concordance with the method considered the gold standard for perforator detection," with a sensitivity and specificity comparable to those of computed tomographic angiography (48). Furthermore, this technology has been refined in recent times so that it is no longer limited to expensive camera systems but can be acquired as a miniature smartphone-compatible thermal imaging camera that currently retails at under €300. It has been the subject of tests in recent studies and provides a low-cost alternative to classic TI while still having a high detection rate (48,49).

In this study, thermal imaging was conducted using the FLIR One® Pro for iOS attachment for iOS Smartphones (FLIR Systems, Inc., USA) (c.f. *Section 2.4*).

1.5.2 Hyperspectral imaging

Like thermal cameras, (hyper-)spectral cameras also capture electromagnetic radiation but are not restricted specifically to emitted infrared wavelengths. Spectral cameras can capture an electromagnetic spectrum, which is defined as the totality of emitted, transmitted, and reflected electromagnetic waves (including light). The particularity of a hyperspectral camera is its ability to capture a separate spectrum for each pixel. This data can be used to create an image that contains thousands to hundreds of thousands of spectra (depending on the image resolution). Electromagnetic spectra provide detailed information about the composition of materials and the sequence of processes (50).

Hyperspectral imaging (HSI) technology has shown promising results in numerous studies testing its use in the medical field—for example, in determining perfusion parameters for diabetic feet (51) or for free flap monitoring (52,53). It provides high-quality information about tissue oxygenation and perfusion. Although this technology has not yet been widely used for perforator mapping, it seems to have significant potential because of its qualities in tissue analysis. Currently, HSI systems are expensive and laborious to use in daily practice because of their size.

The hyperspectral images in this study were created using the TIVITA® Wound (Diaspective Vision GmbH, Germany), which can capture wavelengths from 500nm to 1000nm (c.f. *Section 2.4*).

1.5.3 Laser Doppler imaging

A laser Doppler imaging (LDI) device sends out a narrow and monochromatic light beam onto a tissue surface, where its incident photons penetrate said tissue to a certain depth, depending on its optical properties. If those photons encounter moving particles (e.g., blood cells,) they become Doppler-broadened to a degree determined by the concentration and velocity of the moving scatterers. A fraction of the reflected photons is then captured by a photodetector, which uses this data to create an image, giving information about the state of tissue perfusion (54).

LDI has been successfully used in various medical and surgical fields to identify perfusion patterns (55,56). Furthermore, it can serve as an additional tool to help identify the dominant perforator(s) in flaps (57).

This study used the moorLDLS-BI LaserDoppler (Moor Instruments Ltd., United Kingdom) to execute laser Doppler imaging (c.f. *Section 2.3*). This device is used routinely in burn surgery to assess tissue perfusion and therefore burn depth (58).

2 Materials and methods

This study has already been published by *Nischwitz et al.* in the Journal of Personalized Medicine on the 5th of October 2021, which is hereby referenced (59). Formal or contentual congruencies to the publication might be found in the preceding or following text, which are not marked explicitly.

2.1 Study design

The method employed in this thesis was a prospective, monocentric comparison study as the literature addressing the specific question addressed by this research is scarce. The data collection was performed between June 2020 and August 2020 at the Division of Plastic, Aesthetic and Reconstructive Surgery, Department of Surgery at the Medical University of Graz, Austria. The study protocol was approved by the ethics committee of the Medical University of Graz (31-477 ex 18/19).

2.2 Study cohort

This pilot study included 18 adults who were inpatients at the Division of Plastic, Aesthetic and Reconstructive Surgery between June and August 2020 or healthy individuals who were willing to participate (e.g., the study team).

The main inclusion criteria were defined as:

- Willingness to participate in this study
- Age between 18 and 80 years

The exclusion criteria were:

- Pre-existing micro-circulation compromising conditions such as
    - diabetes mellitus type 1 or type 2
    - vascular diseases, including peripheral arterial disease, aortic aneurysm, current pulmonary embolism, current deep vein thrombosis, or chronic venous insufficiency
- Preceding abdominal surgery
- Presence of scars (originating from surgery or trauma) in the abdominal area
- Current pregnancy
- Current treatment with corticosteroids or other immunosuppressive drugs

These inclusion and exclusion criteria were chosen to ensure the best possible vessel quality and perfusion for detecting the perforators. Subject-related data such

as sex, age, height, weight, abdominal circumference, and body mass index (BMI) were obtained from each subject (cf. *Section 3.1*, *Table 1*). All the obtained information was pseudonymized.

2.3 Detection devices

Thermal imaging

In this study, the thermal imaging was conducted using the FLIR One® Pro for iOS attachment for iOS Smartphones (FLIR Systems, Inc., USA). This device is described as a useful and simple technique in screening for perforator vessels. It can visualize temperature differences of up to 0.07°C, thus displaying more perfused areas (perforators) compared to less perfused areas of the abdominal wall. As demonstrated in *Fig. 8*, it is a handy device connected to a smartphone using the charging socket, making it practical to use. Imaging material was processed with the corresponding FLIR One® app. Detailed specifications of the device are available on the manufacturer's homepage (60).

Figure 8: FLIR One® Pro (60)

Figure 9: TIVITA® Wound (61)

Hyperspectral imaging

For the execution of hyperspectral imaging, the TIVITA® Wound (Diaspective Vision GmbH, Germany) was used (*Fig.9*). This device non-invasively creates color-coded images that provide detailed information about the following tissue factors:

- Tissue oxygen saturation (StO_2)
- Tissue hemoglobin index (THI)
- NIR perfusion index (NIR = near infrared)
- Tissue water index
- Necrotic tissue characteristics

Using the above-mentioned color-coding, a differentiation of well-perfused tissue and the surrounding area can be made. The images were analyzed directly using the affiliated computer program. Detailed specifications of the device are available on the manufacturer's homepage (61).

Figure 10: Moor LDLS-BI LaserDoppler (62)

Laser Doppler imaging

For laser Doppler imaging, the moorLDLS-BI LaserDoppler (Moor Instruments Ltd., United Kingdom) was used (*Fig. 10*). As mentioned in *Section 1.5*, it uses the Doppler shift of laser light reflected off blood cells to create an image that visualizes perfusion patterns. The created images were studied using the affiliated computer program. Detailed specifications of the device are available on the manufacturer's homepage (62).

2.4 Study methods

18 subjects were included in this pilot project and divided into three groups of six subjects each. Each group included two subjects from every age group (18–39 years, 40–59 years, and 60–79 years.) The age limits were chosen due to the limited indication for free perforator flaps especially in older patients.

Following the signed informed consent, the aforementioned subject-related data was collected. The abdominal circumference of participants was measured with a measuring tape by the study team and rounded to the nearest centimeter. For each subject, a region of interest (ROI) was defined as a square of 10x10cm ranging from the umbilicus downwards in the midline (c.f. *Fig 11*). This ROI was chosen due to findings of sufficient perforator vessels in said region in previous DIEP flap

surgeries. Further, the umbilicus provides a gratifying landmark which makes the ROI easily reproducible.

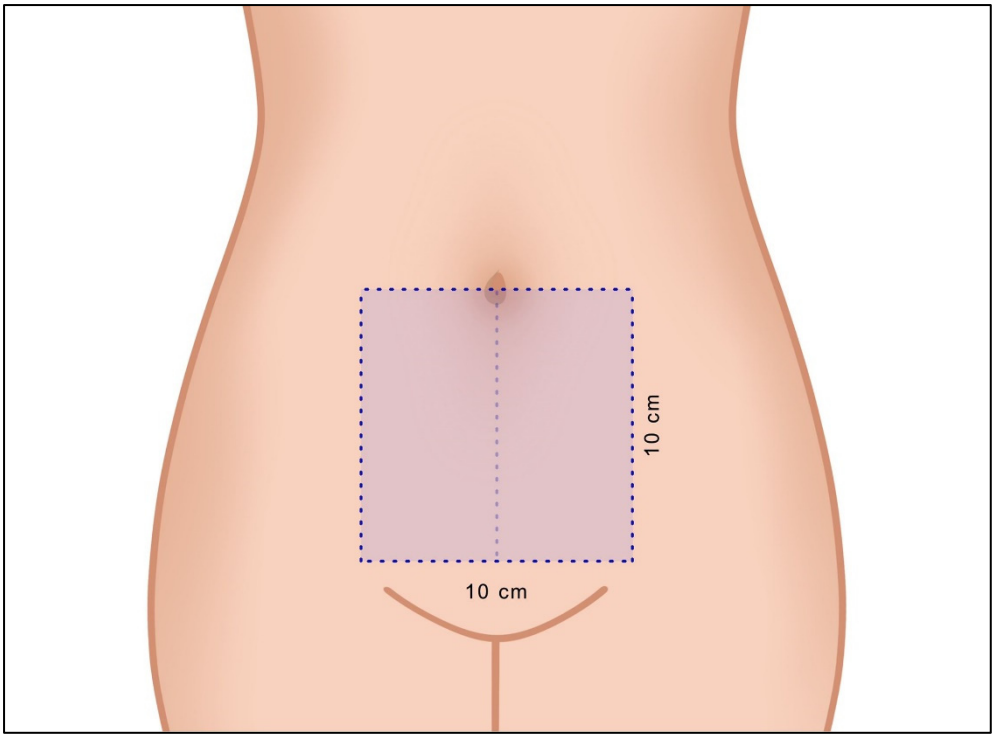

Figure 11: The ROI was defined as a square of 10x10cm ranging from the umbilicus downwards in the midline

Next, a screening for abdominal perforator vessels was carried out within the ROI using a handheld acoustic pencil Doppler.

After the screening, the ROI was cooled using a commercially available cooling pack. This was done to minimize skin perfusion and achieve better contrast in the images. To achieve consistency of temperature of the abdominal skin in all subjects, the cooling pack was stored in a temperature-monitored fridge at 5°C for at least 20 hours before being placed on the ROI for 20 minutes. After that, the cooling pack was removed, and the first imaging was performed. For the following imaging methods, the cooling pack was applied in the same manner, after a cooling break of 60 minutes to regain skin perfusion.

All patients received each imaging method, but in a different order to avoid possible bias by repeated measurements, as follows:

- Group 1 (Patients 1–6) received thermal imaging first, laser Doppler imaging second, and hyperspectral camera imaging last.
- Group 2 (Patients 7–12) received the hyperspectral camera imaging first, thermal imaging second, and laser Doppler imaging last.
- Group 3 (Patients 13–18) received laser Doppler imaging first, hyperspectral camera imaging second, and thermal imaging last.

With each imaging method, an image was captured every 60 seconds for five minutes, starting from the moment the cool pack was removed. This equals six images per imaging method per subject, resulting in 108 images per imaging method. A 60-minute break was scheduled between removal and reapplication of the cooling pack for the next imaging method to regenerate the skin perfusion.

The timeline for the procedure is displayed in *Figures 12–14.*

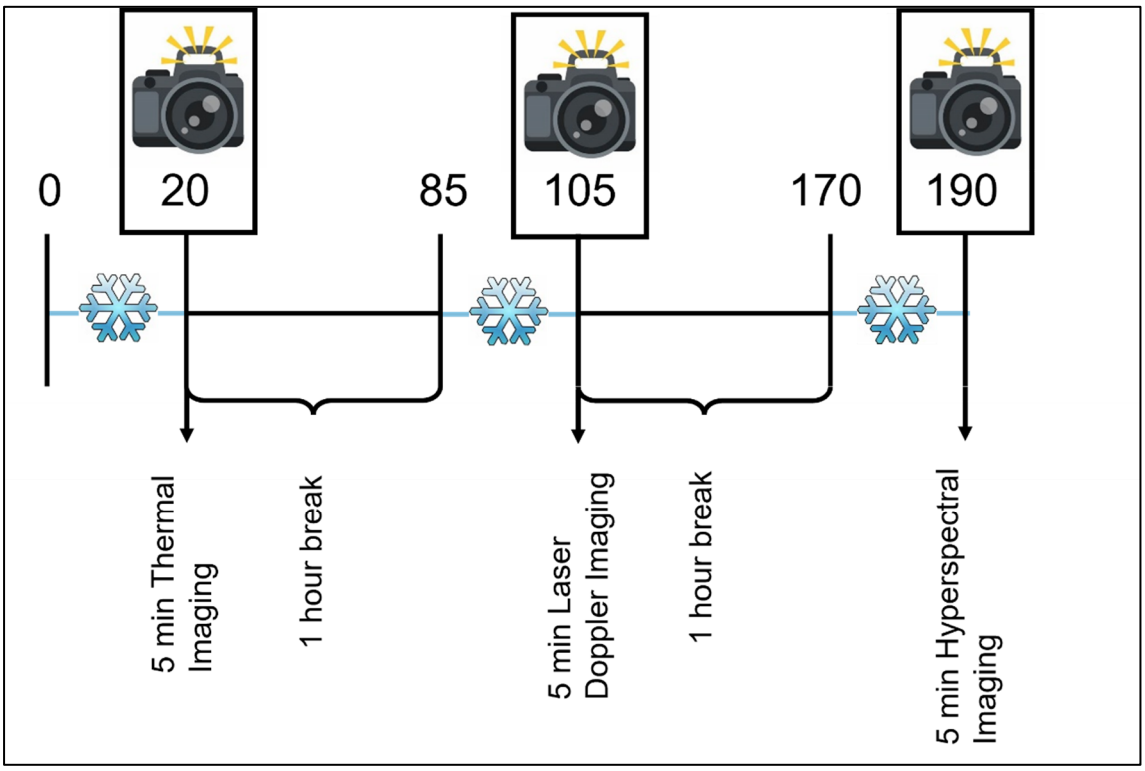

Figure 12: Imaging order group 1: thermal imaging first, laser Doppler imaging second, hyperspectral imaging last. A cooling pack was applied 20 min. before the first imaging and in between the following imaging methods. A break of 1 hour after every imaging method was scheduled.

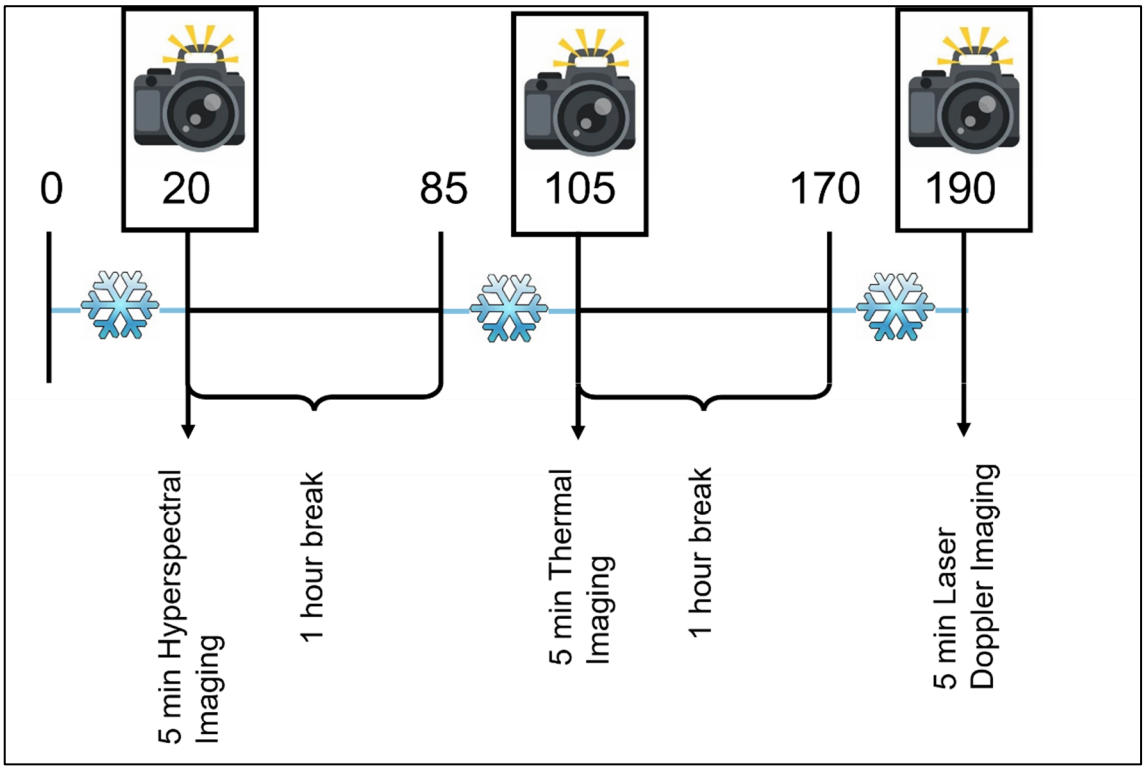

Figure 13: Imaging order group 2: hyperspectral imaging first, thermal imaging second, laser Doppler imaging last. A cooling pack was applied 20 min. before the first imaging and between the following imaging methods. A break of 1 hour after every imaging method was scheduled.

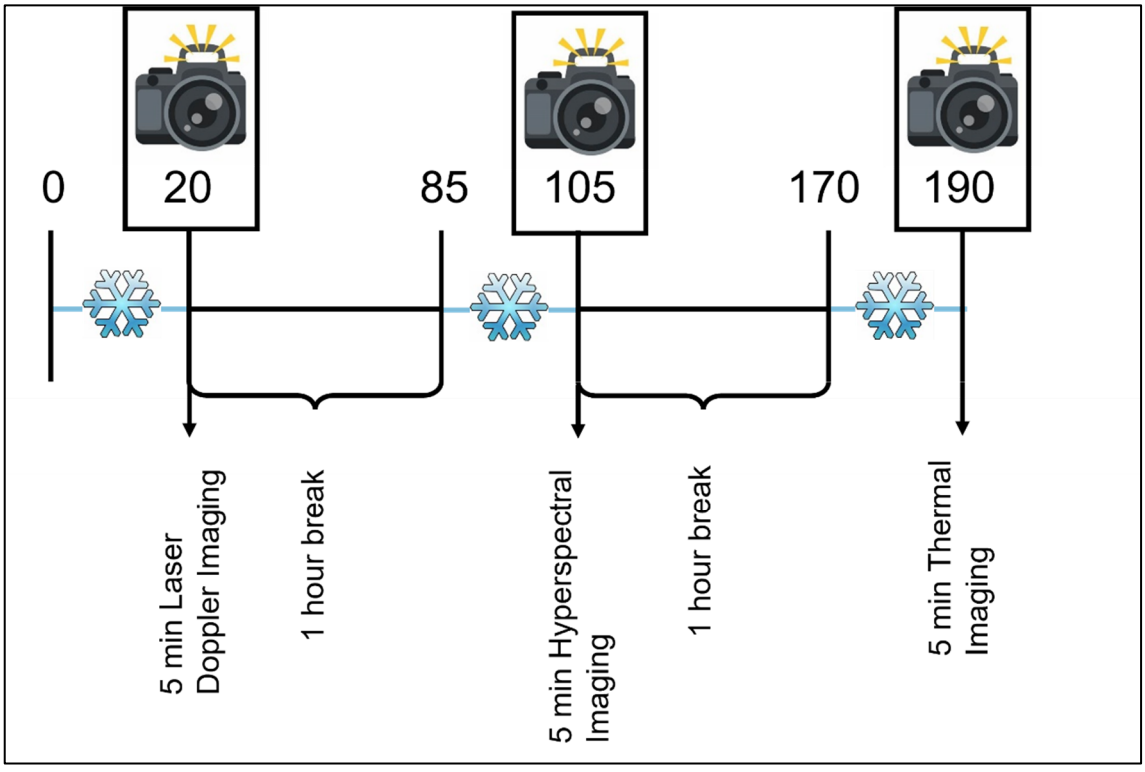

Figure 14: Imaging order group 3: laser Doppler imaging first, hyperspectral imaging second, thermal imaging last. A cooling pack was applied 20 min. before the first imaging and in between the following imaging methods. A break of 1 hour after every imaging method was scheduled.

After the completion of the three imaging methods, the most prominent perforator vessel was identified in each subject using the handheld pencil doppler. This procedure was performed individually by two experienced investigators, who were both plastic surgery residents. To avoid possible bias, neither of the investigators had knowledge of the results of the previous imaging procedure. Each investigator screened the ROI separately and subjectively chose the most prominent perforator in the area. If no concordance could be reached, both were used as further reference.

2.5 Analysis

Following the imaging and the screening process, the images were analyzed according to the previously selected perforators. The ROI in the images was divided into 16 equal squares (4x4). Perforator locations in TI, HSI, and LDI images on one side and the locations of pencil Doppler identification were then compared and matched.

To statistically analyze the results, each image was assigned to one of four possible cases:

1. True positive: In this case, the reference perforator could clearly be seen on the image.
2. False positive: Another perforator that was distinctly more prominent than the reference perforator could be seen in the image.
3. True negative: No perforator was visible in the image and no reference perforator could be detected previously.
4. False negative: No perforator could be seen in the image, but a reference perforator could be detected previously.

2.5.1 Statistical analysis

For each imaging technology, specificity, sensitivity, and false positive and negative rates were calculated in correlation with the detection of perforators using the handheld pencil Doppler device. Using a one-way analysis of variance (one-way ANOVA), differences between the groups were determined. The Pearson correlation coefficient was used to determine a correlation between patient related characteristics and a possible perforator identification. The level of significance was set to $p < 0.05$.

3 Results

3.1 Subject data

As mentioned in *Section 2.4*, body data was collected from each subject prior to the imaging procedure. The subjects were assigned to three groups so that each group included two subjects of each age range (18–39, 40–59, 60–79). Therefore, no significant difference in age could be determined between the three groups (p=0.76).

Furthermore, there was no significant difference regarding sex (p=0.34), BMI (p=0.30), or abdominal girth (p=0.27).

The male to female ratio in the 18 subjects was 2:1. The age ranged from 22 to 71 years, with a mean of 46.06 years.

Only 16 subjects could be statistically analyzed for the body data, as two participants had missing data. The mean BMI for the 16 subjects was 26.37, ranging from 19.13 to 34.72. The height ranged from 155cm to 192cm, with a mean of 173.5cm, while the mean weight was 79.8kg, ranging from 54kg to 108kg.

Regarding the definition of the reference perforators using a handheld acoustic pencil Doppler device after the imaging procedure, at least one perforator vessel could be identified in each subject. In six cases, a perforator could be detected on both sides. The location sides of the other 12 subjects were partitioned in a left-to-right ratio of 3:1 (nine left, three right).

Table 1: Data of the study population

Subject ID	Sex	Age [years]	BMI [kg/m²]	Abdominal girth [cm]	Perforator detection
01	Male	36	m.d.	m.d.	Left
02	Male	30	22.86	78	Right
03	Male	58	29.30	111	Right
04	Male	41	32.53	108	Left
05	Male	65	m.d.	m.d.	Left
06	Female	71	27.89	92	Left + Right
07	Female	28	23.88	82	Left + Right
08	Female	22	19.13	68	Left
09	Female	52	23.44	70	Left + Right
10	Male	41	31.56	102	Left
11	Male	61	22.21	92	Left + Right
12	Male	62	23.66	93	Left
13	Male	24	25.98	92	Left
14	Female	24	20.44	70	Left
15	Male	49	32.77	132	Right
16	Female	45	34.72	110	Left
17	Male	60	26.47	100	Left + Right
18	Male	60	25.08	98	Left + Right
Total /mean (SD)	66.6% Male 33.3% Female	46.1 (+/-15.5)	26.37 (+/-4.53)	93.63 (+/-16.84)	9 Left, 3 Right 6 Left + Right

Abbreviations: missing data (m.d.); standard deviation (SD)

3.2 Overview

A total of 324 images was taken, which equals 108 images per imaging method or 18 images per subject. In 128 images, the identified perforator could be unequivocally matched, representing a success rate of 39.51%.

However, none of the aforementioned body parameters influenced the detection rate, regardless of the technology. Furthermore, no correlation was found between the sequence of the different imaging methods and the detection rate. *Figure 15* displays the detection rate of perforator vessels for each imaging technology.

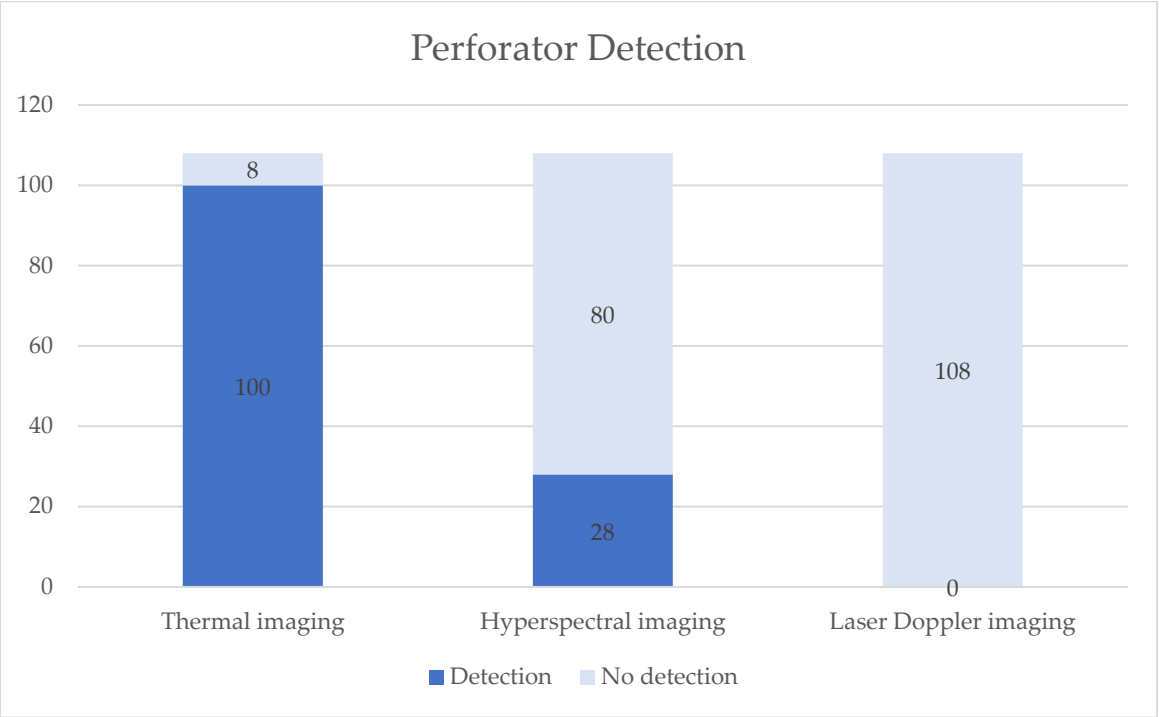

Figure 15: Summary of the detection results of the three imaging methods: For each imaging method, 108 images were captured. Using TI, 100 images (92.59%) showed the reference perforator vessel. With HSI, the vessel was detected in 28 images (25.93%). In LDI, none of the images displayed the reference perforator.

3.3 Thermal imaging results

A matching perforator could be identified in 100 of the 108 images taken, which equals a sensitivity of 92.59%. In 16 of the 18 subjects, the regarding perforator vessel could be identified in all six images taken. In one subject, a perforator vessel could not be identified in any of the six images. In another subject, the matching perforator slowly emerged and could be identified after two minutes for four images. There was no possible detection in eight of the 108 images, although the previous pencil Doppler screening was successful. This represents a false negative rate of 7.41%.

However, no false positive perforator vessels were detected, which equals a specificity of 100%. *Figure 16* displays an exemplary depiction of a marked perforator using TI.

There was no statistically relevant correlation between BMI, abdominal circumference, age or sex and a possible perforator detection via TI – respective p-values are shown in *Table 2.*

Table 2: No significant correlation between body parameters and possible perforator detection via TI could be shown.

	BMI (n=16)	Abdominal Circumference (n=16)	Age (n=18)	Sex (n=18)
p-value	0.93	0.93	0.16	0.50

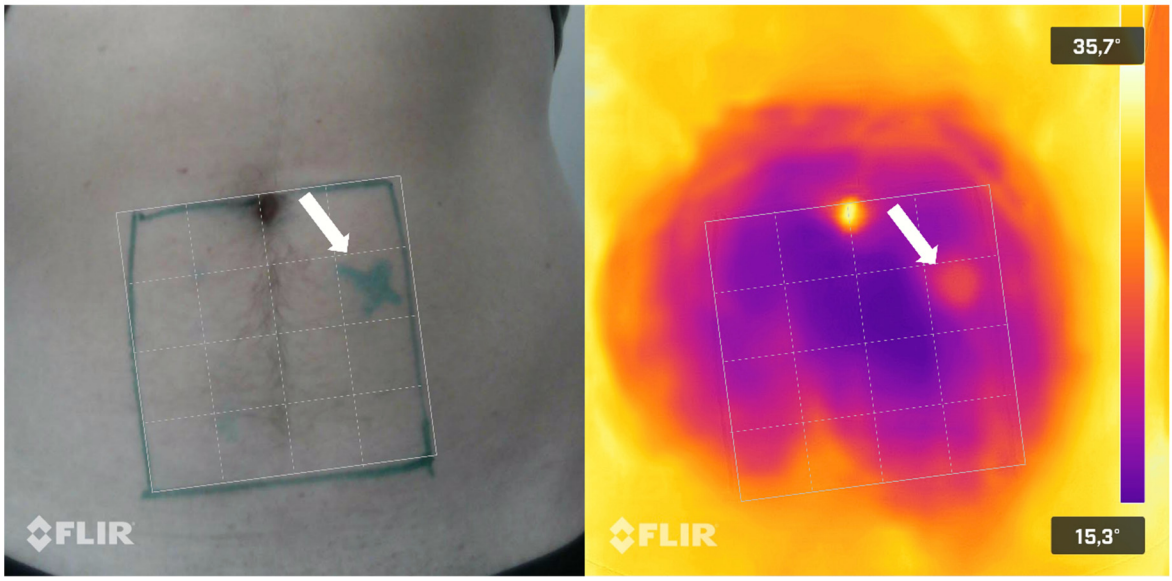

Figure 16: Exemplary depiction of a marked perforator (left arrow) and the corresponding perforator in the TI (infrared) image (right arrow)

3.4 Hyperspectral imaging results

Using HSI, 28 of 108 images showed a positive correlation between the depicted and the reference perforator, equaling a sensitivity of 25.93%. The 28 positive images related to seven patients, as follows:

- In three patients, the reference perforator was visible in all six images.
- In two patients, the reference perforator was visible in the first three images (for two minutes).
- In two patients, the reference perforator was visible in the first two images (for one minute).

However, in 11 patients, no perforator could be identified. This equals a false negative rate of 74.07%. Since no false positive perforator was detected, the result

is a mathematical specificity of 100%. *Figure 17* shows an exemplary hyperspectral image with a matching perforator.

No statistically relevant correlation between BMI, abdominal circumference, age or sex and a possible perforator detection via HSI could be observed – respective p-values as shown in *Table 3*.

Table 3: No significant correlation between body parameters and possible perforator detection via HSI could be shown.

	BMI (n=16)	Abdominal Circumference (n=16)	Age (n=18)	Sex (n=18)
p-value	0.84	0.67	0.09	0.52

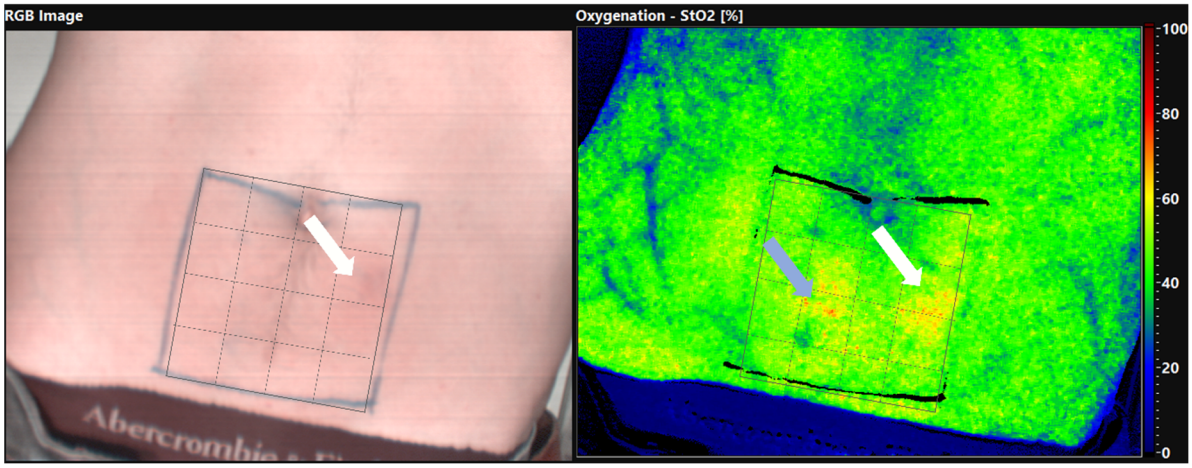

Figure 17: Exemplary depiction of a marked perforator (left, white arrow) and the corresponding perforator in the HSI (oxygenation StO2) image (right, white arrow). The mark has been removed and is visible as a pale area to avoid interfering with the HSI. The gray arrow shows another possible perforator that had not been referenced with the pencil Doppler; it was not distinctly more prominent than the reference perforator.

3.5 Laser Doppler imaging results

It was not possible to detect a reference perforator vessel in any of the 108 images taken, let alone any perforator vessel. Therefore, this technique provides a sensitivity of 0% and, mathematically, a specificity of 100%, as there were no false positive perforators.

An exemplary depiction with no clearly visible reference perforator is shown in Figure 18.

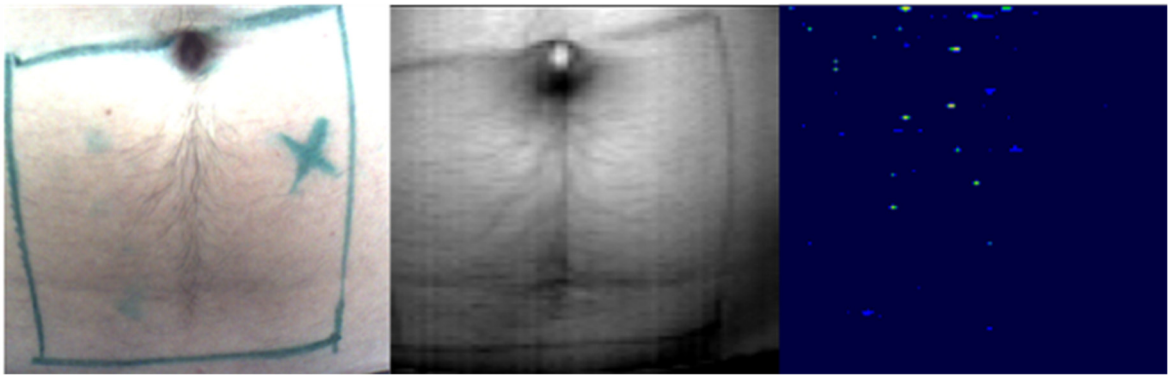

Figure 18: Exemplary depiction of a marked perforator (left, green x) and the corresponding LDI images, where no perforator was detectable.

4 Discussion

This study investigated three non-invasive imaging methods and their ability to detect perforator vessels in the abdominal wall. The main aim was to discover whether any of these technologies could serve as an alternative or additional screening method to a CT angiography, which is the current gold standard in preoperative perforator detection. The investigated imaging methods were compared to the handheld pencil Doppler, the standard addition to CT angiography at the conducting institution. The reason for this was the applicability of this screening method to any patient compared to the limiting factors of CT angiography (e.g., allergy to iodine).

However, with the handheld pencil Doppler, it cannot accurately be assessed whether a perforator is dominant and how much surface area it provides with blood, as the sound emitted by the probe does not correlate with the size of the perforator (63). Furthermore, the screening of false positive locations cannot be ruled out because signals from deep blood vessels that do not necessarily perfuse the skin are received in some situations. Additionally, the handheld pencil Doppler's diagnostic value strongly depends on the examiner and their routine when using this device.

The three tested imaging technologies—thermal imaging, hyperspectral imaging, and laser Doppler imaging—have been previously assessed in different clinical studies and different indications, however have not been compared to each other regarding their ability to detect abdominal perforator vessels yet. This study yields promising and clinically relevant results, which are discussed in the following sections.

4.1 The use of thermal imaging in the medical field

TI has been increasingly used in the medical field in the last 20 years. Its possible use ranges from the detection of postoperative infections (64) to the evaluation of burn depth (65–67), and intraoperative or postoperative free flap monitoring (68). To date, several clinical studies verify the clinical relevance and benefits of TI in different indications:

Romanò et al. (2011) investigated temperature changes of the knee after total knee replacement surgery (64). In 40 patients with uncomplicated surgery a mean temperature difference of 4.4 ± 0.6 °C was found comparing the surgical site area

to the healthy knee on postoperative day three (highest temperature difference in the follow up). Within 90 days post-op, the mean difference in temperature gradually fell to zero (baseline), showing a temperature regularity of healing surgical wounds. The same study also found a significantly elevated mean temperature difference in patients with septic complications, making TI a helpful tool in diagnostics of postoperative wound infections.

Apart of the detection of postoperative complications, TI may also be used in burn surgery: *Xue et al. (2018)* compared TI using the FLIR One to indocyanine green imaging regarding the ability to determine burn extent in five patients with third degree burns (66). The two investigated techniques showed an overlap of more than 90% in the determined areas. However, the FLIR One® overestimated the margin of unsalvageable tissue by approximately 1-2cm. Nevertheless, TI is a promising and price-effective complement in determination of third degree burn extent.

The use of TI in preoperative perforator detection has been only investigated in a few studies so far. *Rabbani et al. (2020)* used the FLIR One® to screen for perforators in a total of 184 patients (154 scheduled for pedicled flap surgery and 30 for free flap surgery) (69). To verify the findings obtained in the screening, perioperative visual inspection was set as gold standard. The results showed a sensitivity of 86.2% and a specificity of 80%.

Another comparable study conducted by *Pereira et al.* (mentioned in *Section 1.5.1*) achieved a sensitivity of 100% and a specificity of 98% comparing the FLIR One® TI to a conventional CT angiography. The subject cohort in this study included 20 patients with 38 screened anterior lateral thigh (ALT) flap regions.

4.2 Thermal imaging in the present study

In our study, the TI detection rate reached a sensitivity of 92.59% and a specificity of 100% compared to the acoustic pencil Doppler device.

The minor differences in the sensitivity and specificity rates to the studies mentioned above appear to depend on the reference detection technology that it is compared to and the methods of evaluation.

In the procedure of our study, a 20-minute period of skin cooling was implemented before each imaging method. The reason for this was to visualize the dynamic

reperfusion of the abdominal wall and therefore be able to identify dominant perforators more easily. This approach was proposed by *Weum et al. (2016)* (70).
Hardwicke et Skillman (2016) found out that "patients may not be happy to undergo a cold challenge during their clinical consultation or preoperative assessment" (71). However, in our study, none of the patients reported the cold challenge as uncomfortable or an impairment during their clinical stay. Similar experiences were found by *de Weerd et al*. *(2014)*, who added, that the recovery phase after the cold challenge is vital for the detection of a suitable perforator vessel, as they are more assessable in this dynamic phase (63). In our study, the goal of sufficiently inhibiting the abdominal skin perfusion using cooling packs, thus showing the dynamic of reperfusion, could not be reached. Only one subject showed a perforator vessel that successively perfused more tissue over time, whereas in all the other participants, the reference perforator was shown immediately after removal of the cooling pack.
Therefore, the FLIR One® shows a high detection rate in our study and should at least complement the current screening methods of abdominal perforators. the present study could show no correlation between sex, age, BMI, abdominal circumference, and a possible detection, so TI can be used in almost any patient and is a viable alternative option for patients unable to undergo a CT angiography.

4.2.1 Practicability of the FLIR One®

The FLIR One® thermal imaging device showed exceptionally simple and intuitive user-friendliness, requiring almost no training. Furthermore, its acquisition costs are substantially lower (currently €209.00 on the FLIR One website) than those of the other tested devices and current standards. Another highlighting factor is its versatility is its handy dimensions (34 x 67 x 14mm), which allow medical staff to create thermal images of almost any location in a matter of seconds.
The FLIR One® comes in a small protection case which fits easily in every pocket of regular hospital clothing or scrubs. Another advantage of the device is its reliability. Environmental factors such as low light or inconsistent temperature do not affect its imaging quality, whereas the other two tested devices are susceptible to those factors. As a result, the FLIR One® can uncomplicatedly be used in almost every environment, making it perfect for quick and easy bedside imaging.
As mentioned in *Section 2.3,* it is connected to a smartphone via the charging port. During the use of the camera, it uses the screen of the connected device to portray a real time preview of the image. On the side of the screen a color-coded

temperature scale shows the temperature range in the image. During and after image acquisition markers can be placed anywhere in the image to show the exact punctual surface temperature.
Further, the FLIR One® is able to record thermal videos. With a frame rate of 8.7Hz it seems a bit jerky compared to normal cameras. However, in future studies the video recording feature could be useful, for example to create time lapse footage showing the reperfusion of the abdominal tissue trough perforator vessels after skin cooling.

4.3 The use of hyperspectral imaging in the medical field

HSI is non-invasive and can visualize certain processes and compositions in different tissues (c.f. *Section 1.5.2*). This unique combination led to a number of different uses in the medical field, some of which are described below.
Most of the named studies also used a TIVITA® hyperspectral camera which provides various blood flow and substance parameters as well as additional tissue information, including tissue oxygen saturation (StO_2) to assess superficial perfusion, the NIR perfusion index to assess deeper perfusion, and the tissue hemoglobin index (THI) that measures the percental volume of hemoglobin of surface perfusion (72).
HSI was for example investigated in the evaluation of PAD (73). *Grambow et al. (2019)* took hyperspectral images of the angiosome of the medial plantar artery in a total of 74 patients (25 healthy and young, 24 with PAD and 25 without PAD in comparable age). The results showed a significantly reduced StO_2 and NIR perfusion index in patients with PAD. Further, those parameters positively correlated with results of the ankle-brachial-index (ABI), vascular quality of life score and the complaint-free walking distance. The authors describe it as promising tool in the screening and follow up for patients with PAD.
HSI could also show promising results in the evaluation and monitoring of different wounds, as a study conducted by *Daeschlein et. al. (2017)* suggests (72).
Another field of use for HSI was investigated by *Sucher et al. (2019)*, who tested the technology on its use to identify resection planes in an anatomical liver resection (74). After occluding the left liver artery and left portal vein, a hyperspectral image clearly showed the segment borders between the left and right liver due to the reduced StO_2 and NIR perfusion index.

These studies proved the excellent quality of HSI in visualization of perfusion patterns. However, regarding the use of HSI in perforator detection, only one comparable study was found during the research for this work. In said study, *Goetze et al*. *(2020)* compared HSI to color-coded ultrasound on the location of perforator vessels in ALT flaps sites (75). Their study achieved an overall sensitivity of 97%. A comparison between *Goetze et al.* and the present study is made in the following section.

4.4 Hyperspectral imaging in the present study

Comparing HSI and TI in the present study, the HSI technology did not match TI regarding perforator detection. Further, the elaborated sensitivity of 25.93% does not reflect the results of the study by *Goetze et al*. mentioned above.

For the imaging procedure, *Goetze et al*. took the images in a time window ranging from directly before applying a cooling pack for three minutes to three minutes after the cooling pack was removed. The highest sensitivity of 98% could be achieved after three minutes of cooling and after one minute of non-cooling reperfusion.

However, in our study, the images were taken after a cooling period of 20 minutes and then each minute for a reperfusion period of five minutes. Two of the investigated subjects showed the reference perforator for one minute after cooling pack removal, and two subjects showed the reference perforator for two minutes after cooling pack removal.

Comparing the present study with the study of *Goetze et al*., it appears that the cooling period in our study might have been too long to detect most perforators in the brief time window of reperfusion.

Another factor that might have influenced the outcome was the use of slightly different imaging devices. While *Goetze et al*. used the TIVITA® Tissue system, the present study conducted the HSI using the TIVITA® Wound system. The two systems come with different software packages that include different focal points.

In conclusion, the encouraging results of *Goetze et al*. could not be reproduced in our study. However, while the ability of hyperspectral cameras to detect perforator vessels needs to be assessed in further studies with a larger subject cohort, it is clear that this technology shows promising results in similar fields of application—for example, in perfusion monitoring of pedicled and free flaps (53,76–78).

4.4.1 Practicability of the TIVITA® Wound hyperspectral camera

Regarding practicability, the TIVITA® Wound, which is connected to a computer on a trolley (c.f. *Fig 9*), is bulky and cannot be transported easily. Further, low light and no movement of the patient is required to receive qualitative imaging results, making it unpractical for bedside imaging. However, the software interface is intuitive, user friendly, and requires almost no training. Nevertheless, with a current price of several thousand euros, it is far more expensive than the TI device.

4.5 The use of laser Doppler imaging in the medical field

As mentioned in *Section 1.5.3*, LDI has been successfully used various medical and surgical fields. Especially in ophthalmology it is a well-studied and broadly used technology. (56,79) Furthermore, LDI is effective in postoperative flap monitoring and the assessment of burn wounds, as shown in studies following below.

Shin et Yi (2016) conducted a systematic literature review and meta-analysis which analyzed the usability of LDI in burn depth assessment. The pooled sensitivity and specificity (89% and 93%) showed a high diagnostic accuracy, making it a helpful tool in this specific field of application (58).

Tindholdt et al. (2011) used LDI to visualize perfusion patterns in DIEP flaps. They divided the flap in four different zones and evaluated the perfusion of these zones preoperatively, perioperatively and postoperatively. Using LDI they successfully visualized the dynamics of perfusion depending on the phase of surgery (80). Similar results have been achieved by *Van den Heuvel et al. (2011)* and *Abdelrahman et al. (2020)* (81,82).

Regarding determination of perfusion patterns in DIEP and TRAM flaps, *Beier et al. (2013)* showed that LDI can be a helpful tool in intraoperative decision-making (57).

The abovementioned studies show that LDI is a useful technology for evaluation of perfusion in many aspects. However, regarding preoperative perforator detection, the present study could not show promising results, as described in the following section.

4.6 Laser Doppler imaging in the present study

In this study, the tested LDI device (moorLDLS-BI) was unable to detect abdominal perforator vessels using the aforementioned cooling protocol. No vessel could be visualized in any of the images taken.

In contrast to this result, a comparable study by *Komuro et al. (2002)* showed a high sensitivity and specificity of LDI in abdominal perforator detection (83). In said study, 10 healthy subjects were screened for abdominal perforators with a LDI device manufactured by Moor Instruments Ltd. The results showed a high correlation with the findings of the pencil Doppler used for confirmation. Comparing the study methods of *Komuro et al.* with those of the present study, it stands out that no cooling protocol was used in the former. Considering this fact, it is possible, that the cooling period of 20 minutes, as performed in our study, could be a factor that led to non-detectability of perforator vessels.

Furthermore, it is not unambiguously clear which exact LDI device was used by *Komuro et al.* Also this fact could have led to the diverging results.

4.6.1 Practicability of the moorLDLS-BI LaserDoppler

Like the tested hyperspectral camera, the moorLDLS-BI LaserDoppler is a bulky device that needs a connection to a computer on a trolley (c.f. *Fig. 10*) and is therefore unpractical in terms of maneuverability and logistics. Furthermore, the software interface requires training as it appears unintuitive and a bit outdated. Additionally, it is temperature sensitive and needs to be calibrated regularly to receive accurate results, which is time-consuming and laborious.

4.7 Limitations and outlook

Since this was a pilot study, only a small number of participants (18 subjects) was included. Hence, it is possible that a potential influence of the repeated measurements could have been concealed. Moreover, none of the participants was scheduled for a DIEP flap surgery, which denied the study team intraoperative visual confirmation of screened perforator vessels.

Even though no correlation between sex and possible detection could be evaluated, the study cohort contained a female to male ratio of 1:2. Given that DIEP flap surgery is mainly performed on women, this fact could have potentially influenced the observed results.

As previously mentioned, the length of the cooling period could have affected the visualization of perforator vessels and, therefore, the resulting sensitivity and specificity of each device.

Another limiting factor was the choice of the ROI, which was defined as a 10x10cm square below the umbilicus. Since the study concentrated on this region, it is possible that potential perforators outside the area could have been overlooked.

In the present study, the imaging technologies were assessed in the context of body parameters such as sex, age, BMI, and abdominal circumference, which showed no correlation. However, future studies could include physical parameters such as blood pressure and body temperature to differentiate possible influential factors further.

Additionally, different cooling strategies and their effect on the sensitivity and specificity of different detection devices should be assessed further. Generally, larger patient cohorts are needed to evaluate these factors more precisely.

5 Conclusion

In the present study, the FLIR One® thermal camera showed impressive results regarding preoperative abdominal perforator detection. With a sensitivity and specificity of over 90% it can thoroughly compete with the use of a pencil Doppler, which is frequently used as an addition to the CT-Angiography at the conducting institution. Its low acquisition cost and easy handling underline its usability. Since the imaging procedure is non-invasive and can be performed bedside in a matter of seconds, it is a viable alternative for patients unable to undergo a CT-scan. Further it can be a helpful addition to established screening methods, for example if the operator is inexperienced in the use of pencil Dopplers or if perfusion patterns are unclear.

Regarding HSI and LDI, the tested devices are not suitable for preoperative perforator detection according to the results of the present study. However, their qualities regarding visualization of perfusion are extent and include postoperative flap-monitoring, evaluation of burn wounds and diagnosis of peripheral vascular diseases, as many of the aforementioned studies suggest.

The preoperative perforator detection is of utmost importance to reduce intra- and postoperative complications. In our opinion, it is recommendable to choose an individual approach for each patient - possibly combining several imaging technologies - to guarantee the most beneficial possible for the patient.

Nevertheless, future studies investigating thermal imaging for perforator detection are mandatory to determine its' full potential.

References

1. Tao ZQ, Shi A, Lu C, Song T, Zhang Z, Zhao J. Breast Cancer: Epidemiology and Etiology. Cell Biochem Biophys. 2015 Jun 15 [cited 2021 Feb 8];72(2):333–8. Available from: https://pubmed.ncbi.nlm.nih.gov/25543329/
2. IARC. Age standardized (World) Incidence Rates, Breast, All ages. Int Agency Res Cancer, WHO. 2021 [cited 2021 Aug 31];876:1–2. Available from: https://gco.iarc.fr/today%0Ahttps://gco.iarc.fr/today%0Ahttp://gco.iarc.fr/today
3. Siegel RL, Miller KD, Jemal A. Cancer statistics, 2019. CA Cancer J Clin. 2019 Jan [cited 2021 Aug 31];69(1):7–34. Available from: https://pubmed.ncbi.nlm.nih.gov/30620402/
4. Lyman GH, Greenlee H, Bohlke K, Bao T, DeMichele AM, Deng GE, et al. Integrative therapies during and after breast cancer treatment: ASCO endorsement of the SIO clinical practice guideline. J Clin Oncol. 2018 Sep 1;36(25):2647–55.
5. American Society of Clinical Oncology (ASCO). Breast Cancer: Types of Treatment | Cancer.Net. Cancer.net. 2020 [cited 2021 Sep 1]. p. 1–20. Available from: https://www.cancer.net/cancer-types/breast-cancer/types-treatment
6. Jahkola T, Asko-Seljavaara S, Von Smitten K. Immediate breast reconstruction. Scand J Surg. 2003 [cited 2021 Oct 15];92(4):249–56. Available from: https://pubmed.ncbi.nlm.nih.gov/14758913/
7. Burgess C, Cornelius V, Love S, Graham J, Richards M, Ramirez A. Depression and anxiety in women with early breast cancer: Five year observational cohort study. Br Med J. 2005 Mar 26 [cited 2021 Oct 15];330(7493):702–5. Available from: https://pubmed.ncbi.nlm.nih.gov/15695497/
8. Arroyo JMG, López MLD. Psychological Problems Derived from Mastectomy: A Qualitative Study. Int J Surg Oncol. 2011 [cited 2021 Oct 15];2011:1–8. Available from: https://pubmed.ncbi.nlm.nih.gov/22312492/
9. Benditte-Klepetko H, Koller R, Ptak-Butta J, Deutinger M. Psychosoziale aspekte der brustrekonstruktion. Geburtshilfe Frauenheilkd. 2003 Jan 1

[cited 2021 Mar 22];63(1):37–42. Available from: http://www.thieme-connect.de/DOI/DOI?10.1055/s-2003-37094

10. Headon H, Kasem A, Mokbel K. Capsular contracture after breast augmentation: An update for clinical practice. Arch Plast Surg. 2015 Sep 1 [cited 2021 Sep 2];42(5):532–43. Available from: https://pubmed.ncbi.nlm.nih.gov/26430623/
11. Fracon S, Renzi N, Manara M, Ramella V, Papa G, Arnež ZM. Patient satisfaction after breast reconstruction: Implants vs. autologous tissues. Acta Chir Plast. 2017 [cited 2021 Sep 2];59(3–4):120–8. Available from: https://pubmed.ncbi.nlm.nih.gov/29651851/
12. Rose J, Puckett Y. Breast Reconstruction Free Flaps. StatPearls. 2019 [cited 2021 Sep 1]; Available from: http://www.ncbi.nlm.nih.gov/pubmed/31082092
13. Opsomer D, Vyncke T, Depypere B, Stillaert F, Blondeel P, Van Landuyt K. Lumbar Flap versus the Gold Standard: Comparison to the DIEP Flap. Plast Reconstr Surg. 2020 [cited 2021 Sep 1];145(4):706E-714E. Available from: https://pubmed.ncbi.nlm.nih.gov/32221200/
14. Teunis T, Van Voss MRH, Kon M, Van Maurik JFMM. CT-angiography prior to diep flap breast reconstruction: A systematic review and meta-analysis. Vol. 33, Microsurgery. Microsurgery; 2013 [cited 2020 Oct 19]. p. 496–502. Available from: https://pubmed.ncbi.nlm.nih.gov/23836386/
15. Gunderman RB, editor. Essential Radiology. Essential Radiology. Stuttgart: Georg Thieme Verlag; 2014 [cited 2020 Oct 18]. Available from: http://www.thieme-connect.de/products/ebooks/book/10.1055/b-002-92682
16. Hallock GG. Direct and indirect perforator flaps: The history and the controversy. Plast Reconstr Surg. 2003 Feb [cited 2021 Aug 22];111(2):855–66. Available from: https://pubmed.ncbi.nlm.nih.gov/12560714/
17. Blondeel PN, Van Landuyt KHI, Monstrey SJM, Hamdi M, Matton GE, Allen RJ, et al. The “Gent” consensus on perforator flap terminology: Preliminary definitions. Plast Reconstr Surg. 2003 [cited 2021 Aug 22];112(5):1378–82. Available from: https://pubmed.ncbi.nlm.nih.gov/14504524/
18. Noone RB, Murphy JB, Spear SL, Little JW. A 6-year experience with immediate reconstruction after mastectomy for cancer. Plast Reconstr Surg.

1985 [cited 2021 Mar 23];76(2):258–69. Available from: https://pubmed.ncbi.nlm.nih.gov/2991957/

19. Eberlein TJ, Crespo LD, Smith BL, Hergrueter CA, Douville L, Eriksson E. Prospective evaluation of immediate reconstruction after mastectomy. Ann Surg. 1993 [cited 2021 Mar 23];218(1):29–36. Available from: https://pubmed.ncbi.nlm.nih.gov/8328826/
20. American Society of Plastic Surgeons. Plastic Surgery Statistics | American Society of Plastic Surgeons. Plastic Surgery Statistics . 2019 [cited 2021 Aug 17]. Available from: https://www.plasticsurgery.org/news/plastic-surgery-statistics
21. Salibian AA, Frey JD, Karp NS. Strategies and considerations in selecting between subpectoral and prepectoral breast reconstruction. Gland Surg. 2019 Feb 1 [cited 2021 Sep 2];8(1):11–8. Available from: /pmc/articles/PMC6378251/
22. Liu J, Hou J, Li Z, Wang B, Sun J. Efficacy of Acellular Dermal Matrix in Capsular Contracture of Implant-Based Breast Reconstruction: A Single-Arm Meta-analysis. Aesthetic Plast Surg. 2020 Jun 1 [cited 2021 Aug 17];44(3):735–42. Available from: https://pubmed.ncbi.nlm.nih.gov/31919627/
23. Implant Reconstruction Reconstruction on Long Island, New York | Dr. Tanna. [cited 2021 Aug 17]. Available from: https://www.breastflap.com/breast-reconstruction/options/implant-reconstruction/
24. Ricci JA, Epstein S, Momoh AO, Lin SJ, Singhal D, Lee BT. A meta-analysis of implant-based breast reconstruction and timing of adjuvant radiation therapy. J Surg Res. 2017 Oct 1 [cited 2021 Aug 17];218:108–16. Available from: https://pubmed.ncbi.nlm.nih.gov/28985836/
25. Kelley BP, Ahmed R, Kidwell KM, Kozlow JH, Chung KC, Momoh AO. A systematic review of morbidity associated with autologous breast reconstruction before and after exposure to radiotherapy: Are current practices ideal? Ann Surg Oncol. 2014 [cited 2021 Aug 17];21(5):1732–8. Available from: https://pubmed.ncbi.nlm.nih.gov/24473643/
26. Koshima I, Soeda S. Inferior epigastric artery skin flaps without rectus abdominis muscle. Br J Plast Surg. 1989 [cited 2021 Aug 19];42(6):645–8.

Available from: https://pubmed.ncbi.nlm.nih.gov/2605399/
27. Healy C, Allen RJ. The evolution of perforator flap breast reconstruction: Twenty years after the first DIEP flap. J Reconstr Microsurg. 2014 Feb [cited 2021 Aug 19];30(2):121–6. Available from: https://pubmed.ncbi.nlm.nih.gov/24163223/
28. Gray Henry. Gray, Henry. 1918. Anatomy of the Human Body. . 2000 New York: Bartleby. 2000 [cited 2021 Aug 19]. Available from: https://www.bartleby.com/107/
29. Buntic R. The deep inferior epigastric artery perforator (DIEP) flap. 2021 [cited 2021 Aug 19]. Available from: https://www.microsurgeon.org/diep
30. Bank J, Pavone LA, Seitz IA, Roughton MC, Schechter LS. CASE REPORT Case Report and Review of the Literature: Deep Inferior Epigastric Perforator Flap for Breast Reconstruction After Abdominal Recontouring.. Vol. 12, Eplasty. 2012 [cited 2021 Aug 19]. p. e52. Available from: https://www.researchgate.net/publication/234106323_CASE_REPORT_Case_Report_and_Review_of_the_Literature_Deep_Inferior_Epigastric_Perforator_Flap_for_Breast_Reconstruction_After_Abdominal_Recontouring
31. Darcy CM, Smit JM, Audolfsson T, Acosta R. Surgical technique: The intercostal space approach to the internal mammary vessels in 463 microvascular breast reconstructions. J Plast Reconstr Aesthetic Surg. 2011 Jan [cited 2021 Aug 20];64(1):58–62. Available from: https://pubmed.ncbi.nlm.nih.gov/20542484/
32. Arnez ̌ZM, Valdatta L, Tyler MP, Planins ̌ek F. Anatomy of the internal mammary veins and their use in free TRAM flap breast reconstruction. Br J Plast Surg. 1995 [cited 2021 Aug 20];48(8):540–5. Available from: https://pubmed.ncbi.nlm.nih.gov/8548153/
33. Vila I, Couto-González I, Brea-García B. Basic Principles in Microvascular Anastomosis and Free Tissue Transfer. Vasc Biol - Sel Mech Clin Appl. 2020 Apr 6 [cited 2021 Aug 20]; Available from: https://www.intechopen.com/chapters/71675
34. DIEP Flap Reconstruction and Technique. In: Bostwick's Plastic and Reconstructive Breast Surgery. 4th ed., Chapter 53, Georg Thieme Verlag; 2020. p. 1389.
35. Edsander-Nord Å, Jurell G, Wickman M. Donor-site morbidity after pedicled

or free TRAM flap surgery: A prospective and objective study. Plast Reconstr Surg. 1998 Oct [cited 2021 Sep 3];102(5):1508–16. Available from: https://pubmed.ncbi.nlm.nih.gov/9774004/

36. Kroll SS, Schusterman MA, Reece GP, Miller MJ, Robb G, Evans G. Abdominal wall strength, bulging, and hernia after tram flap breast reconstruction. Plast Reconstr Surg. 1995 [cited 2021 Sep 3];96(3):616–9. Available from: https://pubmed.ncbi.nlm.nih.gov/7638285/
37. Lohasammakul S, Turbpaiboon C, Ratanalekha R, Lohsiriwat V, Chaiyasate K, Roham A, et al. Anatomy of superficial inferior epigastric vessels: revival of superficial inferior epigastric (SIEA) flap. Eur J Plast Surg. 2018 Aug 22 [cited 2021 Aug 18];41(3):317–24. Available from: https://link.springer.com/article/10.1007/s00238-017-1349-0
38. Lotempio MM, Allen RJ. Breast reconstruction with SGAP and IGAP flaps. Plast Reconstr Surg. 2010 Aug [cited 2021 Oct 15];126(2):393–401. Available from: https://pubmed.ncbi.nlm.nih.gov/20679825/
39. Jo T, Jeon DN, Han HH. The PAP Flap Breast Reconstruction: A Practical Option for Slim Patients. J Reconstr Microsurg. 2021 [cited 2021 Aug 18]; Available from: https://pubmed.ncbi.nlm.nih.gov/33853125/
40. Hammond DC. Latissimus Dorsi Flap Breast Reconstruction. Clin Plast Surg. 2007 Jan [cited 2021 Aug 19];34(1):75–82. Available from: https://pubmed.ncbi.nlm.nih.gov/17307073/
41. Boehmler JH, Butler CE. Latissimus dorsi flap breast reconstruction. Aesthetic Reconstr Surg Breast. 2010 Aug [cited 2021 Aug 19];25(1):51–60. Available from: https://pubmed.ncbi.nlm.nih.gov/29334788/
42. Planck M. The theory of heat radiation : Planck, Max, 1858-1947 : Free Download, Borrow, and Streaming : Internet Archive. The theory of heat radiation. 1914 [cited 2021 Aug 22]. Available from: https://archive.org/details/theoryofheatradi00planrich
43. Gauci J, Falzon O, Formosa C, Gatt A, Ellul C, Mizzi S, et al. Automated Region Extraction from Thermal Images for Peripheral Vascular Disease Monitoring. J Healthc Eng. 2018 [cited 2021 Oct 20];2018. Available from: /pmc/articles/PMC6311825/
44. Lahiri BB, Bagavathiappan S, Jayakumar T, Philip J. Medical applications of infrared thermography: A review. Infrared Phys Technol. 2012 Jul [cited

2021 Oct 20];55(4):221–35. Available from: https://pubmed.ncbi.nlm.nih.gov/32288544/

45. Georgiade NG, Georgiade N, Thorne F. A clinical evaluation of the use of thermography in determining degree of burn injury. Plast Reconstr Surg. 1966 [cited 2021 Oct 20];38(6):512–8. Available from: https://pubmed.ncbi.nlm.nih.gov/5929048/
46. De Weerd L, Miland ÅO, Mercer JB. Perfusion dynamics of free DIEP and SIEA flaps during the first postoperative week monitored with dynamic infrared thermography. Ann Plast Surg. 2009 Jan [cited 2021 Oct 20];62(1):42–7. Available from: https://pubmed.ncbi.nlm.nih.gov/19131718/
47. Sheena Y, Jennison T, Hardwicke JT, Titley OG. Detection of perforators using thermal imaging. Plast Reconstr Surg. 2013 Dec [cited 2020 Oct 19];132(6):1603–10. Available from: https://pubmed.ncbi.nlm.nih.gov/24281586/
48. Pereira N, Valenzuela D, Mangelsdorff G, Kufeke M, Roa R. Detection of perforators for free flap planning using smartphone thermal imaging: A concordance study with computed tomographic angiography in 120 perforators. Plast Reconstr Surg. 2018 [cited 2020 Oct 19];141(3):787–92. Available from: https://pubmed.ncbi.nlm.nih.gov/29481410/
49. Hardwicke JT, Osmani O, Skillman JM. Detection of perforators using smartphone thermal imaging. Plast Reconstr Surg. 2016 Jan 1 [cited 2020 Oct 19];137(1):39–41. Available from: https://pubmed.ncbi.nlm.nih.gov/26710006/
50. Chang C. Hyperspectral imaging: techniques for spectral detection and classification. 2003;378.
51. Greenman RL, Panasyuk S, Wang X, Lyons TE, Dinh T, Longoria L, et al. Early changes in the skin microcirculation and muscle metabolism of the diabetic foot. Lancet. 2005 Nov 12 [cited 2021 Aug 23];366(9498):1711–7. Available from: https://pubmed.ncbi.nlm.nih.gov/16291064/
52. Lu G, Fei B. Medical hyperspectral imaging: a review. J Biomed Opt. 2014 Jan 20 [cited 2021 Aug 23];19(1):010901. Available from: https://pubmed.ncbi.nlm.nih.gov/24441941/
53. Holmer A, Tetschke F, Marotz J, Malberg H, Markgraf W, Thiele C, et al. Oxygenation and perfusion monitoring with a hyperspectral camera system

for chemical based tissue analysis of skin and organs. Physiol Meas. 2016 Oct 27 [cited 2020 Oct 19];37(11):2064–78. Available from: https://pubmed.ncbi.nlm.nih.gov/27786164/

54. Isaka S, Sebald A V. Control strategies for arterial blood pressure regulation. IEEE Trans Biomed Eng. 1993 Apr [cited 2021 Aug 23];40(4):309–16. Available from: https://pubmed.ncbi.nlm.nih.gov/8375866/
55. Hellmann AR, Hać S, Kostro J, Hellmann M, Ledziński Z. The use of the laser-doppler method in surgery. Pol Prz Chir Polish J Surg. 2015 Mar 1 [cited 2021 Aug 23];86(12):604–8. Available from: https://pubmed.ncbi.nlm.nih.gov/25803062/
56. Puyo L, Paques M, Atlan M. Reverse contrast laser Doppler holography for lower frame rate retinal and choroidal blood flow imaging. Opt Lett. 2020 Jul 15 [cited 2021 Aug 23];45(14):4012. Available from: https://pubmed.ncbi.nlm.nih.gov/32667342/
57. Beier JP, Horch RE, Arkudas A, Dragu A, Schmitz M, Kneser U. Decision-making in DIEP and ms-TRAM flaps: The potential role for a combined laser Doppler spectrophotometry system. J Plast Reconstr Aesthetic Surg. 2013 Jan [cited 2020 Oct 19];66(1):73–9. Available from: https://pubmed.ncbi.nlm.nih.gov/23017936/
58. Shin JY, Yi HS. Diagnostic accuracy of laser Doppler imaging in burn depth assessment: Systematic review and meta-analysis. Burns. 2016 Nov 1 [cited 2021 Aug 23];42(7):1369–76. Available from: https://pubmed.ncbi.nlm.nih.gov/27215151/
59. Nischwitz SP, Luze H, Schellnegger M, Gatterer SJ, Tuca AC, Winter R, et al. Thermal, hyperspectral and laser doppler imaging: Non-invasive tools for detection of the deep inferior epigastric artery perforators—a prospective comparison study. J Pers Med. 2021 Oct 1 [cited 2021 Nov 4];11(10). Available from: https://pubmed.ncbi.nlm.nih.gov/34683146/
60. FLIR ONE Pro Thermal Imaging Camera for Smartphones | Teledyne FLIR. [cited 2021 Aug 22]. Available from: https://www.flir.eu/products/flir-one-pro/
61. TIVITA® Wound - Diaspective Vision. [cited 2021 Aug 23]. Available from: https://diaspective-vision.com/en/produkt/tivita-wound/
62. Laser Doppler Line Scanning - moorLDLS-BI - Moor Instruments. [cited 2021 Aug 23]. Available from:

https://www.moorclinical.com/products/imaging/line-imaging/

63. De Weerd L, Weum S, Mercer JB. Locating perforator vessels by dynamic infrared imaging and flow doppler with no thermal cold challenge. Ann Plast Surg. 2014 Feb [cited 2021 Sep 5];72(2):261. Available from: https://pubmed.ncbi.nlm.nih.gov/23241758/
64. Romanò CL, Logoluso N, Dell'Oro F, Elia A, Drago L. Telethermographic findings after uncomplicated and septic total knee replacement. Knee. 2012 Jun [cited 2021 Sep 5];19(3):193–7. Available from: https://pubmed.ncbi.nlm.nih.gov/21441031/
65. Ganon S, Guédon A, Cassier S, Atlan M. Contribution of thermal imaging in determining the depth of pediatric acute burns. Burns. 2020 Aug 1 [cited 2021 Sep 5];46(5):1091–9. Available from: https://pubmed.ncbi.nlm.nih.gov/31864785/
66. Xue EY, Chandler LK, Viviano SL, Keith JD. Use of FLIR ONE Smartphone Thermography in Burn Wound Assessment. Ann Plast Surg. 2018 Apr 1 [cited 2021 Sep 5];80(4):S236–8. Available from: https://pubmed.ncbi.nlm.nih.gov/29489530/
67. Jaspers MEH, Carrière ME, Meij-de Vries A, Klaessens JHGM, van Zuijlen PPM. The FLIR ONE thermal imager for the assessment of burn wounds: Reliability and validity study. Burns. 2017 Nov 1 [cited 2021 Sep 5];43(7):1516–23. Available from: https://pubmed.ncbi.nlm.nih.gov/28536040/
68. Just M, Chalopin C, Unger M, Halama D, Neumuth T, Dietz A, et al. Monitoring of microvascular free flaps following oropharyngeal reconstruction using infrared thermography: first clinical experiences. Eur Arch Oto-Rhino-Laryngology. 2016 Sep 1 [cited 2021 Sep 5];273(9):2659–67. Available from: https://pubmed.ncbi.nlm.nih.gov/26385810/
69. Rabbani M, Ilyas A, Rabbani A, Abidin Z, Tarar M. Accuracy of Thermal Imaging Camera in Identification of Perforators. J Coll Physicians Surg Pakistan. 2020 May 1 [cited 2021 Sep 5];30(05):512–5. Available from: https://pubmed.ncbi.nlm.nih.gov/32580849/
70. Weum S, Lott A, De Weerd L. Detection of Perforators Using Smartphone Thermal Imaging. Plast Reconstr Surg. 2016 Nov 1 [cited 2021 Sep 5];138(5):938e-940e. Available from:

https://pubmed.ncbi.nlm.nih.gov/27783018/
71. Hardwicke JT, Skillman JM. Reply: Detection of Perforators Using Smartphone Thermal Imaging. Plast Reconstr Surg. 2016 Nov 1 [cited 2021 Sep 5];138(5):940e. Available from: https://pubmed.ncbi.nlm.nih.gov/27783019/
72. Daeschlein G, Langner I, Wild T, Von Podewils S, Sicher C, Kiefer T, et al. Hyperspectral imaging as a novel diagnostic tool in microcirculation of wounds. Clin Hemorheol Microcirc. 2017 [cited 2021 Nov 10];67(3–4):467–74. Available from: https://pubmed.ncbi.nlm.nih.gov/28885215/
73. Grambow E, Dau M, Sandkuhler NA, Leuchter M, Holmer A, Klar E, et al. Evaluation of peripheral artery disease with the TIVITA® Tissue hyperspectral imaging camera system. Clin Hemorheol Microcirc. 2019 [cited 2021 Nov 10];73(1):3–17. Available from: https://pubmed.ncbi.nlm.nih.gov/31561343/
74. Sucher R, Athanasios A, Köhler H, Wagner T, Brunotte M, Lederer A, et al. Hyperspectral Imaging (HSI) in anatomic left liver resection. Int J Surg Case Rep. 2019 Jan 1 [cited 2021 Nov 10];62:108–11. Available from: https://pubmed.ncbi.nlm.nih.gov/31493663/
75. Goetze E, Thiem DGE, Gielisch MW, Kämmerer PW. Identification of cutaneous perforators for microvascular surgery using hyperspectral technique – A feasibility study on the antero-lateral thigh. J Cranio-Maxillofacial Surg. 2020 Nov 1 [cited 2021 Sep 5];48(11):1066–73. Available from: https://pubmed.ncbi.nlm.nih.gov/32994154/
76. Schulz T, Marotz J, Stukenberg A, Reumuth G, Houschyar KS, Siemers F. Hyperspectral imaging for postoperative flap monitoring of pedicled flaps. Handchirurgie Mikrochirurgie Plast Chir. 2020 Aug 1 [cited 2021 Sep 6];52(4):316–24. Available from: https://pubmed.ncbi.nlm.nih.gov/32823364/
77. Thiem DGE, Frick RW, Goetze E, Gielisch M, Al-Nawas B, Kämmerer PW. Hyperspectral analysis for perioperative perfusion monitoring—a clinical feasibility study on free and pedicled flaps. Clin Oral Investig. 2021 Mar 1 [cited 2021 Sep 6];25(3):933–45. Available from: https://pubmed.ncbi.nlm.nih.gov/32556663/
78. Kohler LH, Köhler H, Kohler S, Langer S, Nuwayhid R, Gockel I, et al. Hyperspectral Imaging (HSI) as a new diagnostic tool in free flap monitoring

for soft tissue reconstruction: a proof of concept study. BMC Surg. 2021 Dec 1 [cited 2021 Sep 6];21(1). Available from: https://pubmed.ncbi.nlm.nih.gov/33931056/

79. Puyo L, Paques M, Fink M, Sahel J-A, Atlan M. In vivo laser Doppler holography of the human retina. Biomed Opt Express. 2018 Sep 1 [cited 2021 Nov 15];9(9):4113. Available from: https://pubmed.ncbi.nlm.nih.gov/30615709/
80. Tindholdt TT, Saidian S, Pripp AH, Tønseth KA. Monitoring microcirculatory changes in the deep inferior epigastric artery perforator flap with laser doppler perfusion imaging. Ann Plast Surg. 2011 Aug [cited 2021 Sep 6];67(2):139–42. Available from: https://pubmed.ncbi.nlm.nih.gov/21508820/
81. Abdelrahman M, Jumabhoy I, Qiu SS, Fufa D, Hsu CC, Lin CH, et al. Perfusion dynamics of the medial sural artery perforator (MSAP) flap in lower extremity reconstruction using laser Doppler perfusion imaging (LDPI): a clinical study. J Plast Surg Hand Surg. 2020 Mar 3 [cited 2021 Sep 6];54(2):112–9. Available from: https://pubmed.ncbi.nlm.nih.gov/31838935/
82. Van Den Heuvel MGW, Mermans JF, Ambergen AW, Van Der Hulst RRWJ. Perfusion of the deep inferior epigastric perforator flap measured by laser doppler imager. Ann Plast Surg. 2011 Jun [cited 2021 Sep 6];66(6):648–53. Available from: https://pubmed.ncbi.nlm.nih.gov/21233705/
83. Komuro Y, Iwata H, Inoue M, Yanai A. Versatility of scanning laser Doppler imaging to detect cutaneous perforators. Ann Plast Surg. 2002 [cited 2021 Nov 15];48(6):613–6. Available from: https://pubmed.ncbi.nlm.nih.gov/12055430/

Appendix

Publication:

Nischwitz SP, Luze H, Schellnegger M, Gatterer SJ, Tuca A-C, Winter R, et al. Thermal, Hyperspectral, and Laser Doppler Imaging: Non-Invasive Tools for Detection of The Deep Inferior Epigastric Artery Perforators—A Prospective Comparison Study. J Pers Med 2021, Vol 11, Page 1005. 2021 Oct 5 [cited 2021 Oct 20];11(10):1005. Available from: https://www.mdpi.com/2075-4426/11/10/1005/htm